ISSN 2658-3518

LIMNOLOGY & FRESHWATER BIOLOGY

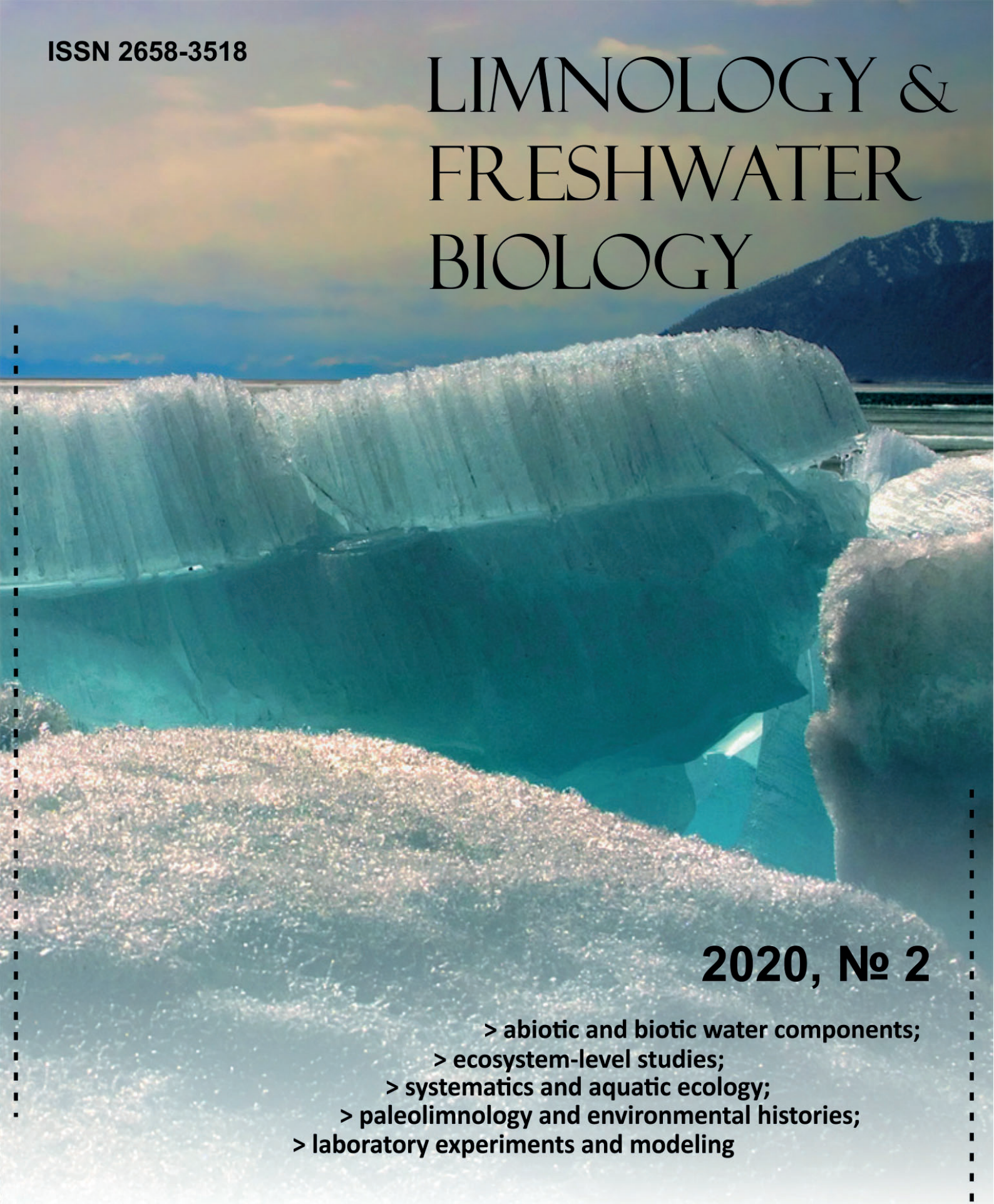

2020, № 2

> abiotic and biotic water components;
> ecosystem-level studies;
> systematics and aquatic ecology;
> paleolimnology and environmental histories;
> laboratory experiments and modeling

Limnology and Freshwater Biology 2020 (2): 382-386 DOI:10.31951/2658-3518-2020-A-2-382

Original Article

ISSN 2658-3518
LIMNOLOGY FRESHWATER BIOLOGY
www.limnolfwbiol.com

Morphological differentiation of the otoliths of graylings from the Barguzin River and Lake Baikal

Anoshko P.N.[1], Dzyuba E.V.[1], Smolin I.N.[1]*, Telpukhovskii A.N.[2], Matveev A.N.[3]

[1] *Limnological Institute, Siberian Branch of the Russian Academy of Sciences, Ulan-Batorskaya Str., 3, Irkutsk, 664033, Russia*
[2] *Angaro-Baikal territorial division of The Federal Agency for Fishery, Smolina Str., 18, Ulan-Ude, 670000, Russia*
[3] *Faculty of Biology and Soil Studies of Irkutsk State University, Sukhe-Batora Str., 5, Irkutsk, 664011, Russia*

ABSTRACT. A comparative analysis of distinctive morphological features of sagittae in the *Thymallus* species from Lake Baikal and the Barguzin River has been done. The otolith shape was described using values of radii and the Fourier descriptors. It is demonstrated that the otoliths of *Thymallus* species have a similar structure. The otolith outline analysis allowed to differentiate the samplings according to the morphotypes that characterize them. No significant differences in length, width, perimeter and area of the otoliths in the *Thymallus* species have been identified. However some differences in the shape of otoliths were described in *T. baicalolenensis*; they had a less developed pararostrum and more salient ventral edge than the otoliths of *T. baicalensis* from the lakes Balan-Tamur and Baikal. The otolith shape analysis can be widely applied for basic research of microevolutionary processes, delimitation of natural populations and preservation of genetic diversity as well as for defining the structure of the commercial stock.

Keywords: *Thymallus*, otolith, shape analysis, catchment area of Lake Baikal

1. Introduction

The otoliths of the teleosts are of great utility for basic studies of fish biology and ecology as well as for fish monitoring. In particular, the sagittae are used to investigate the fish age and growth, population structure and trophic ecology (Ballagh et al., 2006; Rooker et al., 2008). The species specificity of size and morphology of the otoliths finds a use in the fish species identification (Zischke et al., 2016), including the analysis of gastrointestinal content of predatory fish, piscivorous birds and mammals (Furlani et al., 2007). The sizes and morphology of the otoliths underlie identification guides and keys for full-grown fish (Skalkin, 1963; Skazkina, 1965; Yukhov, 1971; Svetocheva et al., 2002) and for young fish (Khrustaleva and Pavlov, 2000). Peculiarities of the variability of otolith size and shape allow to use them for differentiation between closely related species and identification of intraspecific taxa (Campana and Casselman, 1993; Johnson, 1996; Bolles and Begg, 2000; Begg et al., 2001; DeVriesa et al., 2002; Bergenius et al., 2006; Tyagun et al., 2013; Pavlov, 2016).

According to previous studies, the ichthyofauna of the upper Barguzin (Baikal's tributary) catchment area is represented by two species of the genus *Thymallus*: *Thymallus baicalolenensis* Matveev, Samusenok, Pronin & Tel'pukhovsky, 2005 (Matveev et al., 2005; Prosekin, 2007) and *Thymallus baicalensis* Dybowski, 1874 that significantly differs in a number of traits from the *T. baicalensis,* inhabiting Lake Baikal and being its geographical form (Prosekin, 2007). The *T. baicalolenensis* mostly prefers mountainous rivers, while the *T. baicalensis* inhabits mountainous lakes of the Amut relict glacial basin located more than 250 km away the Barguzin estuary.

The objective of the study was to define possibilities of otolith differentiation and to identify the most informative traits of their morphology in the *Thymallus* species from various habitats.

2. Material and methods of research

The sagittae from the collection of the Laboratory of Ichthyology of Limnological Institute, Siberian Branch of the Russian Academy of Sciences: *T. baicalolenensis* (25), *T. baicalensis* from the lakes Balan-Tamur (43) and Baikal sampled during the cruise of 2006 (Fig. 1) were used as study material. The fish was first measured for its standard length (*SL*), then the otoliths were extracted for age determination and further analysis. Each otolith was photographed from the exterior side with regard to its anatomic position. The further measurements were done by means of digital imaging. The otolith outline was projected from the digital image onto the image

*Corresponding author.
E-mail address: ursus.88@mail.ru (I.N. Smolin)

plane using Image-Pro Plus software. The outlines of deviant and defective otoliths were excluded from the analysis. Then the area, perimeter, length and width of the projected outline were calculated. The digitized outline was normalized against its position (straight for the right otolith, in inversed manner for the left one), geometrical center superposed on the origin point (maximum in diameter in line with the coordinate axis) and area (the outline was recalculated against the projected area unit).

The polar coordinates were applied for the outline shape analysis. 60 radii (R_i) through equal (6^0) angles were obtained from origin point for each otolith. The Excel and Statistika 6.0 software was used to analyze the data. The values of radii (R_i) and the Fourier descriptors were taken as test objects (Castonguay et al., 1991).

3. Results

The structural plan of otoliths in all form of graylings is similar (Fig. 2). The otoliths of *Thymallus* species are flat, without curve, the rostrum is long, rounded or tapered. The antirostrum is round. The postrostrum and pararostrum are usually divided. The channel *(sulcus acusticus)* is deep. The exterior surface is irregular. The relief corresponds to its optical structure. According to our data, *T. baicalolenensis* (*SL* 24-32 mm) was 4-6 years old, *T. baicalensis* from Lake Balan-Tamur (*SL* 32-40 mm) was 5-12 years old and the fishes from Lake Baikal (*SL* 15-36 mm) were 3-8 years old. When the otoliths become bigger they show a general trend to change their shape: the outline length to width ratio increases and the *excisura minor* and *excisura major* also grow in size (Fig. 2). Although these trends in larger specimens from Lake Balan-Tamur were not pronounced well.

No significant differences in the length, width, perimeter and the outline area of the otoliths, but distinctive features of their shape were found in the fishes from the study sites. Incremental linear discriminant analysis was used to identify the most informative combination of measurements (R_i) and the Fourier descriptors (A_j). Insertion of variables (R_i) and (A_j) stopped at the steps 23 and 18 respectively given F for insertion equal to 1 (Fig. 3). However in the first case two inserted variables R_{51} and R_{27} allow a 90% classification of the otolith samples among the given groups, the results of the classification plateau at the step 4 after insertion of R_{42} having reached 93% of the level of correct classifications. In the second case, the results plateau at the step 10 after insertion of A_{12} reaching 90% of the level of correct classifications. The further insertion of variables may be considered as less informative in both cases because an ulterior growth of classification percentage is due to the otolith that have a low probability to belong to the a priori given groups.

According to the calculations, square of the Mahalanobis distance (R_i at the step 4 and A_j at the step 10) show a higher level of differences between the otoliths samplings of *T. baicalensis* from Lake Balan-Tamur and *T. baicalolenensis* (Table). The distances from

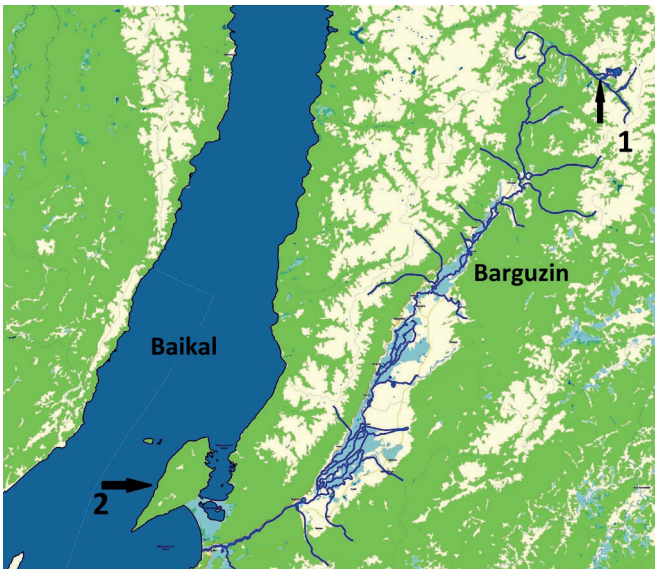

Fig. 1. Sites of the *Thymallus* sampling: 1 – Barguzin River and Lake Balan-Tamur; 2 – Lake Baikal, Svyatoy Nos Peninsula

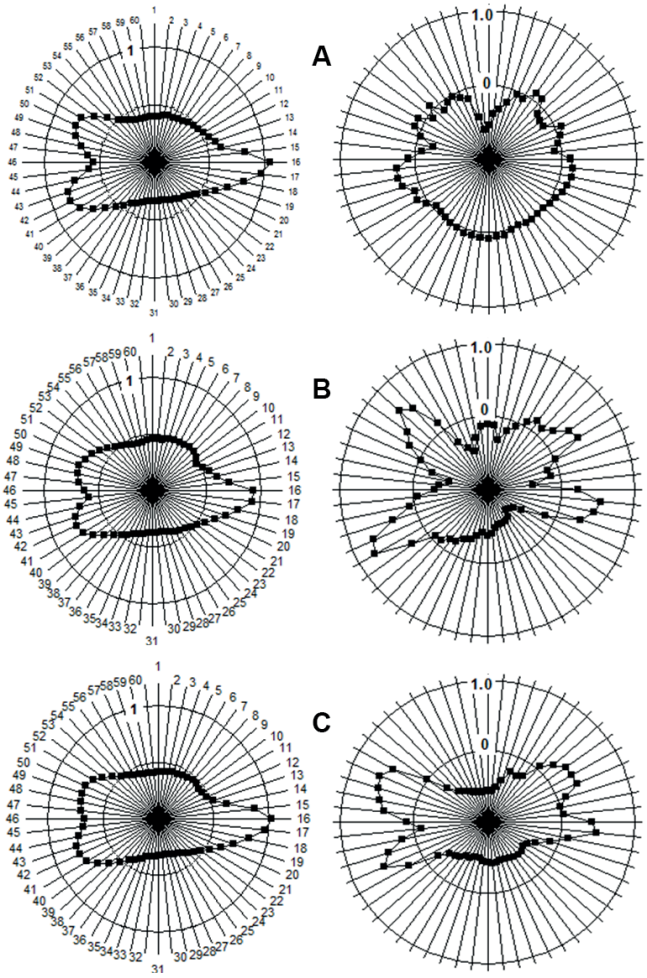

Fig. 2. Diagrams of average values of otolith radii of *T. baicalensis* from Lake Balan-Tamur (A), *T. baicalolenensis* (B), and *T. baicalensis* from Lake Baikal (C) (left panel) and correlation coefficient values against the otolith area (right panel)

the sampling of *T. baicalensis* from Lake Baikal to two other samplings are similar. Thus, the use of the values of radii R_i and the values of the Fourier descriptors A_j in the discriminant analysis yielded the similar results concerning the accuracy of otolith classification and intersample distances.

In coordinates of canonical variables obtained both from R_i and A_j values, the otolith samplings form relatively separate clusters (Fig. 4). As the radii and the descriptors yield the similar results only those based on R_i are given here. Both variables describe a significant proportion of differences: 59 and 41% for the first and the second one, respectively. The value of the first variable depends mostly on R_{51}, while the second one on R_{27}.

The otoliths of *T. baicalolenensis* thus differ in a less developed pararostrum and more convex ventral edge, *T. baicalensis* from Lake Balan-Tamur has otoliths with the least developed pararostrum, while the otoliths of *T. baicalensis* from Lake Baikal have a concave ventral edge. The clusters of other samplings included the otoliths whose morphotype sharply deviated from their group. The shape of these otoliths may be considered deviant for the respective samplings. The sharp deviation from the typical shape, including crystal structure disturbances is of common occurrence in *T. baicalensis* from Lake Baikal (Anoshko et al., 2007). The deviant otoliths were also found in graylings from the Barguzin River and Lake Balan-Tamur. They were thinner, more transparent and lacked a coherent optical structure. It is known that calcium carbonate in such otoliths deposits mostly in the form of vaterite (Gauldie, 1993). However 90% of otoliths have a morphotype characteristic of *Thymallus* species and intraspecific taxa, thus giving a possibility to use them for species identification, e.g. in digestive tracts of predatory fish and piscivorous birds and mammals from the Barguzin catchment area.

4. Discussion and conclusions

The adaptive value of otolith morphological characteristics is unclear (Popper et al., 2005). According to theoretical models there might be differences in the perception of sounds of different frequencies depending on the otolith size (Lychakov and Rebane, 1992; 2000). The intraspecific (and intrapopulation) discrepancies in the otolith morphology may be induced by various reasons or form during the growth as a result of implementation of genetic information under the influence of the environment. A number of papers reports a significant correspondence of the otolith shape to genetic variations on the population level (Jonsdottir et al., 2006; Abuanza et al., 2008; Libungan et al., 2016; Afanasyev et al., 2017). Therefore one may suppose the changes of the otolith shape within specified boundaries could be sporadic. The microevolutionary processes take place on a short-term horizon under the influence both of global and local climatic changes. The otolith morphology as the most morphometric traits is likely a result of expression of many genes.

Table. Square of the Mahalanobis distance between the samplings: *T. baicalensis* from Lake Balan-Tamur (1), *T. baicalolenensis* (2) and *T. baicalensis* from Lake Baikal (3). R_i and A_j are the upper and lower parts of the matrix, respectively

	1	2	3
1		18	11
2	19		12
3	12	14	

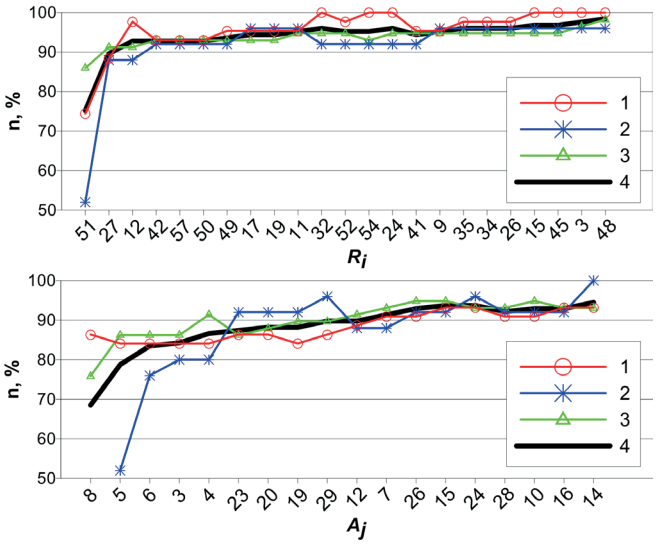

Fig. 3. Results of otolith classification: (1) *T. baicalensis* from Lake Bala-Tamur, (2) *T. baicalolenensis*, (3) *T. baicalensis* from Lake Baikal, (4) all samplings along the stepwise insertion of radii R_i (above) and the Fourier descriptors A_j (below) during the linear discriminant analysis

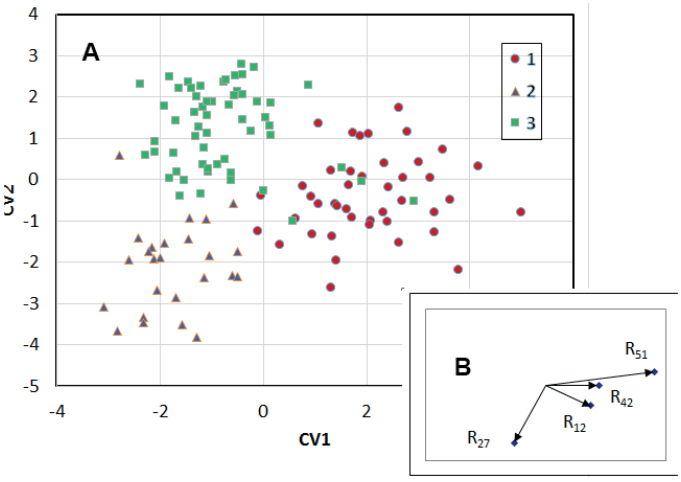

Fig. 4. (A) Differentiation of graylings in coordinates of canonical variables: 1 – *T. baicalensis* from Lake Balan-Tamur, 2 – *T. baicalolenensis*, and 3 – *T. baicalensis* from Lake Baikal. (B) Vectors of factor loadings

Opposed to the morphometric characteristics of fishes, the features of otolith structure depend less on the environment, e.g. short-term changes of the growing period, seasonal action of physical and chemical factors or reproduction cycles (Cadrin and Friedland, 2005). The phenotypical variations of the otoliths do not allow to make conclusions about intraspecific groups of the fishes, however they can evidence that those have been divided for a long time (Campana et al., 1995).

Previously L. Ding and coauthors (Ding et al., 2019) found that the variability of the otoliths of *Schizothorax nukiangensis* Tsao, 1964 could be related to the river dynamics driven by its fall. They showed the otoliths of *S. nukiangensis* sampled in different habitats had a significantly different morphology, in particular they reported an increase of their length. According to Prosekin and Prosekina (Prosekin and Prosekina, 2009) *T. baicalolenensis* and *T. baicalensis* in the Barguzin catchment area inhabit different habitats. *T. baicalensis* gain weight mostly in lakes or in the parts of the river where the stream velocity is less than 1.5 m/s without rapids and shoots. In contrast, *T. baicalolenensis* mainly prefer the river reaches where the stream velocity exceeds 1.5 m/s. In the rare cases when these fishes coinhabit they show a low level of trophic competition as they have different feeding strategies (Prosekin and Prosekina, 2009). However, no significant differences in length and width, perimeter and area of the otoliths between the *Thymallus* species were found during our study. Only the shape of the otoliths had distinctive features: the otoliths of *T. baicalolenensis* had a less developed pararostrum and more convex ventral edge, than those of *T. baicalensis* inhabiting the lakes Balan-Tamur and Baikal.

The studies showed that the otoliths of the *Thymallus* species have a similar structural plan. The analysis of the otolith outline allowed to differentiate the samplings studied pursuant to their typical morphotypes. This analysis has a number of advantages compared to the classical morphological and molecular genetic methods: it is cost effective and allows to quickly obtain primary data for the real time monitoring of population ecology. The otolith shape comparison method could be extensively used for basic research of microevolutionary processes, delimitation of natural populations for the sake of genetic diversity as well as for defining the structure of the commercial stock (Afanasyev et al., 2017).

Acknowledgements

The work was performed within the projects # 0345–2019–0002 and # 0279-2019-0003.

References

Abuanza P., Murta A.G., Campbell N. et al. 2008. Stock identity of horse mackerel (*Trachurus trachurus*) in the Northeast Atlantic and Mediterranean Sea: integrating the results from different stock identification approaches. Fisheries Research 89: 196-209. DOI: 10.1016/j.fishres.2007.09.022

Afanasyev P.K., Orlov A.M., Rolsky A.Yu. 2017. Otolith shape analysis as a tool for species identification and studying the population structure of different fish species. Russian Journal of Zoology 96: 192-200. DOI: 10.1134/S1062359017080027

Anoshko P.N., Telpukhovskiy A.N., Fedorova L.I. et al. 2007. Aberrant otoliths of Baikal grayling. Acta Biomedica Scientifica 2: 10–13. (in Russian)

Ballagh A.C., Begg G.A., Mapleston A. et al. 2006. Growth trends of Queensland east coast Spanish mackerel (*Scomberomorus commerson*) from otolith back-calculations. Marine and Freshwater Research 57: 383-393. DOI: 10.1071/MF05173

Begg G.A., Overholtz W.J., Munroe N.J. 2001. The use of internal otolith morphometrics for identification of haddock stocks on Georges Bank. Fishery Bulletin 99: 1-14.

Bergenius M.A.J., Begg G.A., Mapstone B.D. 2006. The use of otolith morphology to indicate the stock structure of common coral trout (*Plectropomus leopardus*) on the Great Barrier Reef, Australia. Fishery Bulletin 104: 498-511.

Bolles K.L., Begg G.A. 2000. Distinction between silver hake (*Merluccius bilinearis*) stocks in U.S. waters of the northwest Atlantic based on whole otolith morphometrics. Fishery Bulletin 98: 451-462.

Cadrin S.X., Friedland K.D. 2005. Morphometric outlines. In: Cadrin S.X., Friedland K.D., Waldman J.R. (Eds.), Stock identification methods: applications in fisheries science. Amsterdam, pp. 173-183.

Campana S.E., Casselman J.L. 1993. Stock discrimination using otolith shape analysis. Canadian Journal of Fisheries and Aquatic Sciences 50: 1062-1083. DOI: 10.1139/f93-123

Campana S.E., Gagne´ J.A., McLaren J.W. 1995. Elemental fingerprinting of fish otoliths using ID-ICPMS. Marine Ecology Progress Series 122: 115-120. DOI: 10.3354/meps122115

Castonguay M., Simard P., Gagnon P. 1991. Usefulness of Fourier analysis of otolith shape for Atlantic mackerel (*Scomber scombrus*) stock discrimination. Canadian Journal of Fisheries and Aquatic Sciences 48: 269-302. DOI: 10.1139/f91-041

DeVriesa D.A., Grimes C.B., Prager M.H. 2002. Using otolith shape analysis to distinguish eastern Gulf of Mexico and Atlantic Ocean stocks of king mackerel. Fisheries Research 57: 51-62. DOI: 10.1016/S0165-7836(01)00332-0

Ding L., Tao J., Ding C. et al. 2019. Hydrogeomorphic factors drive differences in otolith morphology in fish from the Nu-Salween River. Ecology of Freshwater Fish 28: 132-140. DOI: 10.1111/eff.12437

Gauldie R.W. 1993. Polymorphic crystalline structure of fish otoliths. Journal of Morphology 218: 1-28. DOI: 10.1002/jmor.1052180102

Furlani D., Gales R., Pemberton D. 2007. Otoliths of common Australian temperate fish: a photographic guide. Hobart: CSIRO Publishing.

Johnson A.G. 1996. Use of otolith morphology for separation of king mackrel (*Scomberomorus cavalla*) and Spanish mackerel (*Scomberomorus maculates*). Gulf of Mexico Science 1: 1-6. DOI: 10.18785/goms.1401.01

Jonsdottir I.G., Campana S.E., Marteinsdottir G. 2006. Otolith shape and temporal stability of spawning groups of Icelandic cod (*Gadus morhua* L.). ICES Journal of Marine Science 63: 1501-1512. DOI: 10.1016/j.icesjms.2006.05.006

Khrustaleva A.M., Pavlov D.A. 2000. Features of otolith morphology in the young of several fish species from the White Sea. Journal of Ichthyology 40: 655-667.

Libungan L.A., Slotte A., Otis E.O. et al. 2016. Otolith variation in Pacific herring (*Clupea pallasii*) reflects mitogenomic variation rather than the subspecies classification. Polar Biology 39: 1571-1579. DOI: 10.1007/s00300-015-1882-x

Lychakov D.V., Rebane Y.T. 1992. Effect of otolith shape on directional sound perception in fish. Journal of Evolutionary Biochemistry and Physiology 28: 531-536.

Lychakov D.V., Rebane Y.T. 2000. Otolith regularities. Hearing Research 143: 83-102. DOI: 10.1016/s0378-5955(00)00026-5

Matveev A.N., Samusyonok V.P., Telpukhovsky A.N. et al. 2005. A new subspecies of the Siberian grayling *Thymallus arcticus baicalolenensis* ssp. nova (Salmoniformes, Thymallidae). Vestnik Buryatskogo Gosudarstvennogo Universiteta Seriya 2. Biologiya [Bulletin of the Buryat State

University Series 2. Biology] 7: 69-82. (in Russian)

Pavlov D.A. 2016. Differentiation of three species of the genus *Upeneus* (Mullidae) based on otolith shape analysis. Journal of Ichthyology 56: 37-51. DOI: 10.1134/S0032945216010094

Popper A.N., Ramcharitar J., Campana S.E. 2005. Why otolith? Instings from inner ear physiology and biology. Marine and Freshwater Research 56: 497-504. DOI: 10.1071/MF04267

Prosekin K.A., Prosekina A.A. 2009. To the question on strategy with-existence bajkalolensky and black bajkalsky charius in the conditions of symparion (reserve Dzherginsky). Samarskaya Luka: Problemy Regional'noy i Global'noy Ekologii [Samarskaya Luka: Problems of Regional and Global Ecology 18: 161-164. (in Russian)

Prosekin K.A. 2007. Ecological and biological features of graylings from waterbodies and streams of the upper Barguzin River (Pribaykalye). Cand. Sc. Dissertation, Institute of General and Experimental Biology of the Siberian Branch of the RAS, Ulan-Ude, Russia. (in Russian)

Rooker J.R., Secor D.H., DeMetrio G. et al. 2008. Evidence of trans-Atlantic movement and natal homing of bluefin tuna from stable isotopes in otoliths. Marine Ecology Progress Series 368: 231-239. DOI: 10.3354/meps07602

Skalkin V.A. 1963. Otoliths of some fishes from Far East seas. Proceedings of Pacific Research Institute for Marine Fisheries and Oceanography. 59: 159-200.

Skazkina E.P. 1965. Differences in the otoliths between the Azov Sea and the Black Sea anchovy (*Engraulis encrasicholus maeoticus* Pusanov, *Engraulis encrasicholus ponticus* Aleks.). Journal of Ichthyology 5: 600-605.

Svetocheva O.N., Stasekova N.I., Gosheva T.D. 2002. Otolith morphology of some fishes of the White Sea. Journal of Ichthyology 42: 360-367.

Tyagun M.L., Anoshko P.N., Voronov M.G. 2013. Otolith shape analysis to discriminate among morpho-ecological groups of Baikal omul (*Coregonus migratorius* Georgi). Advances in Limnology 64: 109-118. DOI: 10.1127/1612-166X/2013/0064-0018

Yukhov V.L. 1971. Structure of the otoliths of the Antarctic and the Patagonian toothfish *Dissostichus mawsoni* Norm. and *D. elegenoides* Smitt of the Southern Ocean. Journal of Ichthyology 11: 587-594.

Zischke M.T., Litherland L., Tilyard B.R. et al. 2016. Otolith morphology of four mackerel species (*Scomberomorus* spp.) in Australia: species differentiation and prediction for fisheries monitoring and assessment. Fisheries Research 176: 39-47. DOI: 10.1016/j.fishres.2015.12.003

Limnology and Freshwater Biology 2020 (2): 387-390 DOI:10.31951/2658-3518-2020-A-2-387

Short communication

ISSN 2658-3518
LIMNOLOGY FRESHWATER BIOLOGY
www.limnolfwbiol.com

Study of absorption characteristics of phytoplankton, particles and colored dissolved organic matter in Lake Baikal (July 2018 and September 2019)

Churilova T.[1]*, Moiseeva N.[1], Efimova T.[1], Skorokhod E.[1], Sorokovikova E.[2], Belykh O.[2], Usoltseva M.[2], Blinov V.[2], Makarov M.[2], Gnatovsky R.[2]

[1] O.A.Kovalevski Institute of Biology of the Southern Seas, Russian Academy of Sciences, 2 Nakhimov Ave, Sevastopol, 299011, Russia
[2] Limnological Institute, Siberian Branch of the Russian Academy of Sciences, Ulan-Batorskaya Str., 3, Irkutsk, 664033, Russia

ABSTRACT. Results of two scientific cruises carried out in July 2018 and September 2019 were used for an analysis of variability in spectral bio-optical properties of Lake Baikal. Chlorophyll *a* concentration, spectral light absorption coefficient of phytoplankton, non-algal particles and colored dissolved organic matter varied in ~order of magnitude between stations. Vertical distribution of these bio-optical parameters depended on water column stability in euphotic layer. The chlorophyll *a* profiles were characterized by maximum near the bottom of euphotic zone. In the layer of deep chlorophyll *a* maximum the phytoplankton absorption spectra had a specific feature – a local maximum at 550-570 nm. It was associated with relative increasing of phycoerythrin containing species in phytoplankton community. The absorption budget at 440 nm showed that the CDOM was the main optically active component, which provided ~ 50 % contribution to total absorption on averaged over Lake Baikal surface.

Keywords: phytoplankton, chlorophyll *a*, phycoerythrin, light absorption, non-algal particles, colored dissolved organic matter, Lake Baikal.

1. Introduction

Operative monitoring of the state of unique ecosystem of Lake Baikal can be realized by remote approach. For correct transformation of satellite data to water quality and productivity indicators the development of regional algorithms is required. Spectral absorption properties of phytoplankton, non-algal particles and colored dissolved organic matter are key parameters in bio-optical algorithms. Aim of the research was to investigate spatial and temporal variability in spectral light absorption coefficients of all optically active substances, their link to chlorophyll *a*.

2. Methods

Variability in spectral bio-optical properties of Lake Baikal was investigated in two scientific cruises carried out in July 2018 (RV G.Yu.Vereshagin) and September 2019 (RV G.Titov). Water transparency was assessed based on Secchi disk visibility in July 2018. In September 2019 vertical profiles of temperature, salinity, density, fluorescence (calibrated in dimension of chlorophyll *a* concentration), and photosynthetically available radiation (PAR) were measured by a JFE Rinko AAQ-177 water quality probe (Japan). Pigment concentration was measured by spectrophotometric method (Jeffrey and Humphry, 1975). Spectral absorption by particles ($a_p(\lambda)$) and colored dissolved organic matter ($a_{CDOM}(\lambda)$) were measured in line with the NASA protocol (Boss et al., 2018). To separate the phytoplankton pigments light absorption ($a_{ph}(\lambda)$) and non-algal pigments absorption ($a_{NAP}(\lambda)$) from $a_p(\lambda)$ the pigments were bleached using NaClO 1 % active chloride following the methods of Tassan and Ferrari (1995). For particulate absorption GF/F filters (25 mm diameter) were used. In calculation of particulate absorption, the b-correction was done in line with Mitchell (1990). To determine CDOM absorption water samples were filtered through 47 mm diameter 0.2 μm nucleopore filters using first 50 ml filtered sample for rinsing. Optical density of the samples – particles on the filters and dissolved organic matter were measured with dual-beam spectrophotometer Lambda 35, Perkin Elmer (equipped with integrating sphere) from 350 to 750 nm and from 250 to 750 nm, correspondingly. Fitting of measured $a_{NAP}(\lambda)$ and $a_{CDOM}(\lambda)$ coefficients to exponential function was done for wavelength domain from 400 to 700 nm and

*Corresponding author.
E-mail address: tanya.churilova@ibss-ras.ru (Tanya Churilova)

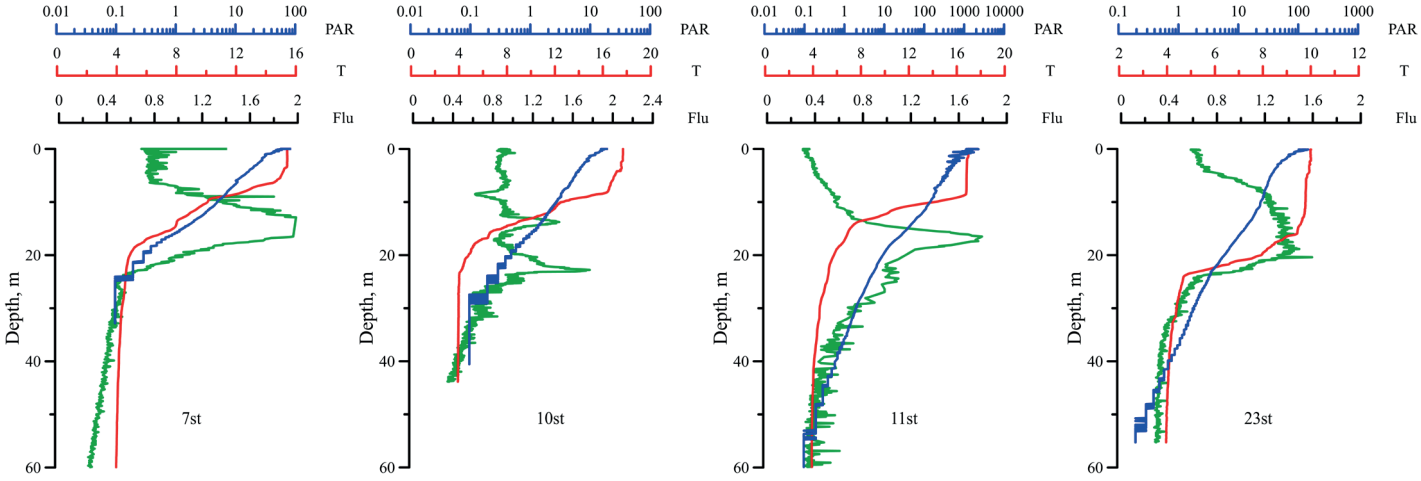

Fig. 1. Vertical profiles of chlorophyll *a* fluorescence (Flu, green line), temperature (T, ºC, red line), photosynthetic available radiation (PAR, μE m^{-2} s^{-1}, blue line) at particular stations in Lake Baikal in September 2019.

from 350 to 500 nm, correspondingly, in accordance with Babin et al. (2003).

3. Results and discussion

Spatial variability of chlorophyll *a* concentration (Chl-*a*), light absorption coefficient of phytoplankton ($a_{ph}(\lambda)$, non-algal particles ($a_{NAP}(\lambda)$) and colored dissolved organic matter ($a_{CDOM}(\lambda)$) was rather high (in order and higher).

In surface layer values of Chl-*a* varied from 0.58 to 5.3 mg m^{-3} in July 2018 and from 0.90 to 2.7 mg m^{-3} in September 2019. Vertical distribution of Chl-*a* was dependent on hydrophysical characteristics, in particular, on temperature stratification of water column (Fig. 1). In situ measured temperature, chlorophyll *a* fluorescence (F) and photosynthetic available radiation (PAR) profiles allowed to analyze Chl-*a* profile types. The upper mixed layer (UML) thickness varied widely (5-20 m) between stations. In case an appearance of the thermocline (TC) within euphotic zone Chl-*a* vertical distribution was characterized by unimodal profile with deep chlorophyll *a* maximum (DCM) in the layer below TC (Fig. 1). The DCM was located near the bottom of euphotic zone (at ~1%PAR). The Chl-*a* in the DCM was in 1.5-6 times higher in comparison to surface layer. The DCM formation is likely to result of an increasing of intracellular chlorophyll *a* concentration in comparison with the surface phytoplankton due to phytoplankton acclimation/adaptation to the environmental factors – mainly to irradiance (Falkowski and Raven, 2007). At a few stations bimodal Chl-*a* profile was observed: second maximum was appeared in TC layer. Deepening of the TC down to the bottom of euphotic zone resulted in relatively homogeneous Chl-*a* distribution within euphotic layer (Fig. 1).

It was shown that water stratification effected on light absorbance capacity of phytoplankton. In the deeper layer of euphotic zone (below the TC) shape of the $a_{ph}(\lambda)$ spectrum has a specific feature – a local maximum at 550-570 nm in comparison to the upper layer absorption spectra (Fig. 2). Light absorbance in the spectral band 550-570 nm is associated with phycoerythrin (PE). The PE-sign became more marked on $a_{ph}(\lambda)$ spectra at depth near the bottom of euphotic zone, where with PAR is low (1-0.1 % of the PAR incident on the lake surface). The appearance of the PE-sign reflects increasing of PE share in total amount of phytoplankton pigments in water, which is associated with increasing of PE-containing species in phytoplankton community. The PE-containing species are likely to be cyanobacteria and eukaryotic algae (Phylum Cryptophyta) with light absorbance bands at ~ 500, ~550 and ~566nm (Moore et al., 1995; Novarino, 2003; Six et al., 2007; Heidenreich and Richardson, 2020). The revealed significant depth-dependent variability in $a_{ph}(\lambda)$ was associated with changes in phytoplankton species composition caused by adaptation of the phytoplankton community to environment, particular to spectral features of downwelling irradiance.

The NAP and CDOM absorption spectra were described by exponential function. The NAP absorption was correlated with phytoplankton absorption: the NAP contribution to particulate light absorption at ~440 nm was ~ 20 % on averaged. The NAP spectra slope coefficient (S_{NAP}) was slightly variable and equal to 0.010 nm^{-1} on averaged, which agreed well with the results from other water areas (Bricaud et al., 1998; Babin et al., 2003; Zhang et al., 2007; Churilova et al., 2017; 2018; Shi et al., 2017;). The CDOM spectra slope coefficient (S_{CDOM}) was 0.018 nm^{-1} on averaged. The analysis of $a_{CDOM}(440)$ and S_{CDOM} variability revealed the relationship between them: the higher values of S_{CDOM} corresponding to the lower values of $a_{CDOM}(440)$ resulted of photo-destruction of high molecular weight compounds to low molecular weight compounds of CDOM (Helms et al., 2008). This type of relationship was in a good agreement with the results observed in the other water areas (Babin et al., 2003; Matsuoka et al., 2012; Churilova et al., 2017; Shi et al., 2017). Parameterization of light absorption by NAP and CDOM revealed no differences between July 2018 and September 2019.

The absorption budget was assessed at the different wavelengths corresponding to satellite

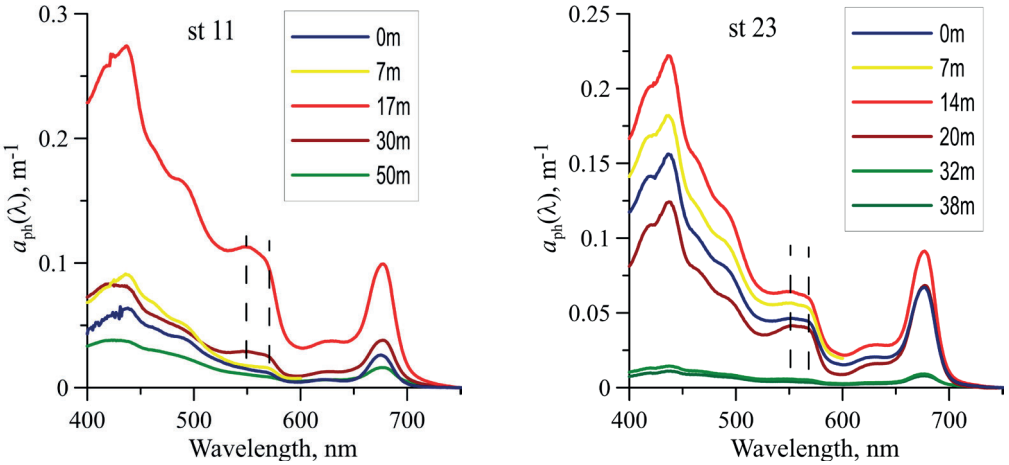

Fig. 2. Phytoplankton light absorption coefficients ($a_{ph}(\lambda)$) at different depths at particular stations in Lake Baikal in September 2019 (dashed black lines are corresponding to 550 and 565 nm).

scanners spectral bands. At the ~440 nm (corresponding to the blue maximum of phytoplankton light absorption spectra) relative contribution of the phytoplankton pigments, NAP and CDOM to total light absorption varied significantly (up to order) between regions of Lake Baikal. The budget at 440 nm showed that the CDOM was the main optically active component, which provided ~ 50 % contribution to total absorption on averaged over Lake Baikal surface. The mean contribution of phytoplankton pigments and NAP to absorption budget at 440 nm was ~38 and ~12 %, correspondingly, without statically reliable difference between years.

4. Conclusions

The obtained new data on variability of spectral light absorption coefficients by phytoplankton, particles and dissolved organic matter, their relation to chlorophyll *a* concentration will be used for analysis of photosynthetic characteristics of phytoplankton, for development of spectral models of downwelling irradiance and primary production with application for remote sensing.

Acknowledgments

The authors are thankful to crews of RV Vereshagin and RV Titov for the help during the sampling. This research was performed in the framework of the state assignment, Russia (theme No. AAAA-A19-119061190081-9).

References

Babin M., Stramski D., Ferrari G.M. et al. 2003. Variations in the light absorption coefficients of phytoplankton, nonalgal particles, and dissolved organic matter in coastal waters around Europe. Journal of Geophysical Research 108. DOI: 10.1029/ 2001JC000882

Boss E., D'Sa E.J., Freeman S. et al. 2018. Ocean optics and biogeochemistry protocols for satellite ocean colour sensor validation. Vol. 1. Inherent optical property measurements and protocols: absorption coefficient. In: Neeley A.R., Mannino A. (Eds.). Dartmouth: IOCCG.

Bricaud A., Morel A., Babin M. et al. 1998. Variations of light absorption by suspended particles with the chlorophyll a concentration in oceanic (case 1) waters: Analysis and implications for bio-optical models. Journal of Geophysical Research 103. DOI: 10.1029/98JC02712

Churilova T., Moiseeva N., Efimova T. et al. 2017. Annual variability in light absorption by particles and colored dissolved organic matter in coastal waters of Crimea (the Black Sea). Proceedings of SPIE: 23rd International Symposium on Atmospheric and Ocean Optics: Atmospheric Physics 10466. DOI: 10.1117/12.2288339

Churilova T., Efimova T., Moiseeva T. et al. 2018. Light absorption by phytoplankton, non-algal particles and colored dissolved organic matter in the Sea of Azov in January and April 2016. Proceedings of SPIE: 24th International Symposium on Atmospheric and Ocean Optics: Atmospheric Physics 10833. DOI: 10.1117/12.2505415

Falkowski P.G., Raven J.A. 2007. Aquatic photosynthesis. Princeton and Oxford: Princeton University Press.

Heidenreich K.M., Richardson T.L. 2020. Photopigment, absorption, and growth responses of marine cryptophytes to varying spectral irradiance. Journal of Phycology 56: 507-520. DOI: 10.1111/jpy.12962

Helms J.R., Stubbins A., Ritchie J.D. et al. 2008. Absorption spectral slopes and slope ratios as indicators of molecular weight, sources, and photobleaching of chromophoric dissolved organic matter. Limnology and Oceanography 53: 955-969. DOI: 10.4319/lo.2008.53.3.0955

Hill D.R.A., Rowan K.S. 1989. The biliproteins of the Cryptophyceae. Phycologia 28: 455-463. DOI: 10.2216/ i0031-8884-28-4-455.1

Jeffrey S.W., Humphrey G.F. 1975. New spectrophotometric equations for determining chlorophylls *a*, *b*, *c*1 and *c*2 in higher plants, algae and natural phytoplankton. Biochemie und Physiologie der Pflanzen [Plant Biochemistry and Physiology] 167: 191-194.

Matsuoka A., Bricaud A., Benner R. et al. 2012. Tracing the transport of colored dissolved organic matter in water masses of the Southern Beaufort Sea: relationship with hydrographic characteristics. Biogeosciences 9: 925-940. DOI: 10.5194/bg-9-925-2012

Mitchell B.G. 1990. Algorithms for determining the absorption coefficient of aquatic particulates using the quantitative filter technique (QFT). Proceedings of SPIE: Ocean Optics X 1302: 137-148. DOI: 10.1117/12.21440

Moore L.R., Georicke R., Chisholm S.W. 1995. Comparative physiology of *Synechococcus* and *Prochlorococcus*: influence of light and temperature on growth, pigments, fluorescence and

absorptive properties. Marine Ecology Progress Series 116: 259-275. DOI: 10.3354/meps116259

Novarino G. 2003. A companion to the identification of cryptomonad flagellates (Cryptophyceae = Cryptomonadea). Hydrobiologia 502: 225-270. DOI: 10.1023/B:HYDR.0000004284.12535.25

Shi L., Mao Z., Wu J. et al. 2017. Variations in spectral absorption properties of phytoplankton, non-algal particles and chromophoric dissolved organic matter in Lake Qiandaohu. Water 9. DOI: 10.3390/w9050352

Six C., Thomas J.-C., Garczarek L. et al. 2007. Diversity and evolution of phycobilisomes in marine *Synechococcus* spp.: a comparative genomics study. Genome Biology 8. DOI: 10.1186/gb-2007-8-12-r259

Tassan S., Ferrari G. 1995. An alternative approach to absorption measurements of aquatic particles retained on filters. Limnology and Oceanography 40: 1358-1368. DOI: 10.4319/lo.1995.40.8.1358

Zhang Y., Zhang B., Wang X. et al. 2007. A study of absorption characteristics of chromophoric dissolved organic matter and particles in Lake Taihu, China. Hydrobiologia 592: 105-120. DOI: 10.1007/s10750-007-0724-4

Limnology and Freshwater Biology 2020 (2): 391-396 DOI:10.31951/2658-3518-2020-A-2-391

Original Article

ISSN 2658-3518
LIMNOLOGY FRESHWATER BIOLOGY
www.limnolfwbiol.com

Water quality in the littoral zone of the Barguzin and Chivyrkuy bays in the summer of 2019

Sakirko M.V.[1]*, Domysheva V.M.[1], Panchenko M.V.[2], Pestunov D.A.[2], Shamrin A.M.[2]

[1] *Limnological Institute, Siberian Branch of the Russian Academy of Sciences, Ulan-Batorskaya Str., 3, Irkutsk, 664033, Russia*
[2] *V.E. Zuev Institute of Atmospheric Optics. Siberian Branch, Russian Academy of Science (IAO SB RAS), Academician Zuev Square Str.,1, Tomsk 634055, Russia*

ABSTRACT. Currently, with an increase in technological progress, anthropogenic impact on the environment is increasingly apparent. Since surface waters are the most vulnerable part of the natural environment, a detailed study of water pollution is one of the urgent tasks. This article presents the results of the instrumental measurements and the assessment of the pollution of the surface waters in the littoral zone of the Barguzin and Chivyrkuy bays of Lake Baikal. To determine the degree of water pollution, we compared hydrochemical indicators with the standards of the maximum permissible concentrations. We revealed that in different parts of the Chivyrkuy Bay, water quality varies in a wide range from slightly polluted to very polluted and, in some cases, highly polluted. The waters in the Barguzin Bay can mainly be classified as slightly polluted, and only in some areas – as moderately polluted or highly polluted. According to the comprehensive water pollution index, the waters in the Chivyrkuy and Barguzin bays is assessed as conditionally polluted and conditionally pure, respectively.

Keywords: Chivyrkuy Bay, Barguzin Bay, Lake Baikal, water quality, nutrients, nitrogen, phosphorus, silica, organic matter, chlorophyll *a*

1. Introduction

Barguzin and Chivyrkuy are the largest bays of Lake Baikal, with an area of 725 and 300 km^2, respectively. They are located on the east coast of Lake Baikal and separated by the Svyatoy Nos Peninsula. The Barguzin valley adjacent to the bay and coves of the Chivyrkuy Bay are known for their mineral springs and attractive to many tourists. All this leads to an increase in anthropogenic pressure on coastal ecosystems and, consequently, ecological problems.

Recent studies have shown that the main problem of Lake Baikal is continuing eutrophication of coastal waters and annual mass development of spirogyra and potentially toxic cyanobacteria that may have a toxic effect on fish and other hydrobionts (Kravtsova et al., 2012; 2014; Timoshkin et al., 2016). In the future, this situation may also occur in the deep part of Lake Baikal.

This study aims to assess the water quality in the Barguzin and Chivyrkuy bays based on the data on the chemical composition of water in the littoral zone.

2. Material and methods

Hydrochemical investigations were carried out in August 2019 on the Barguzin River, at eight stations in the Barguzin Bay and nine stations in the Chivyrkuy Bay (Fig. 1). Sampling was carried out at the locations of settlements, mass recreation of tourists, mooring of ships, the confluence of rivers as well as background coastal areas and in the central parts of the bays. At the central station in the Barguzin Bay, the depth was 150 m; in the Chivyrkuy Bay – 5 m. To compare the data obtained in the central part of the bays with the coastal ones, the depths of 0 and 5 m were used. At each station, samples were taken from the water edge and surface as well as at the bottom at a distance from the coast where the depth was 5 m.

For chemical analyses, certified methods were used. Immediately after collection, pH (regulatory guide RD 52.24.495-2017, 2017) and dissolved oxygen (regulatory guide RD 52.24.419-2005, 2004) were measured in samples. The primary production and destruction of organic matter were determined by the light and dark bottle method (Rukovodstvo…, 1983).

To determine nutrient concentrations, samples were filtered through a membrane filter with a pore size of 0.45 μm. The silica concentrations were determined by the photometric method in a yellow form of molybdosilic acid (regulatory guide RD 52.24.433-2005, 2005). Spectrophotometrically, nitrite ions were determined with Griess reagent (national standard GOST 33045-2014, 2019), ammonium ions

*Corresponding author.
E-mail address: sakira@lin.irk.ru (M.V. Sakirko)

– by the indophenol method (regulatory guide RD 52.24.383-2018, 2018), nitrate ions – using sodium salicylate (national standard GOST 33045-2014, 2019), phosphate ions – with the formation of phosphorus molybdenum blue (national standard GOST 18309-2014, 2015). The concentration of the total phosphorus was determined after conversion of organically bound phosphorus compounds to orthophosphate through high-temperature persulfate oxidation (national standard GOST 18309-2014, 2015).

Chemical oxygen demand (COD) determined by dichromate oxidation (federal environmental regulation PND F 14.1:2:4.190-03, 2007), biochemical oxygen demand (BOD5) (regulatory guide RD 52.24.420-2006, 2006) and permanganate oxidation (federal environmental regulation PND F 14.1:2:4.154-99, 2012) served as indirect indicators of the organic matter content.

The chlorophyll *a* concentration, a photosynthetic pigment characterizing a degree of phytoplankton development, was determined by the spectrophotometric method after acetone extraction (national standard GOST 17.1.4.02-90, 2010).

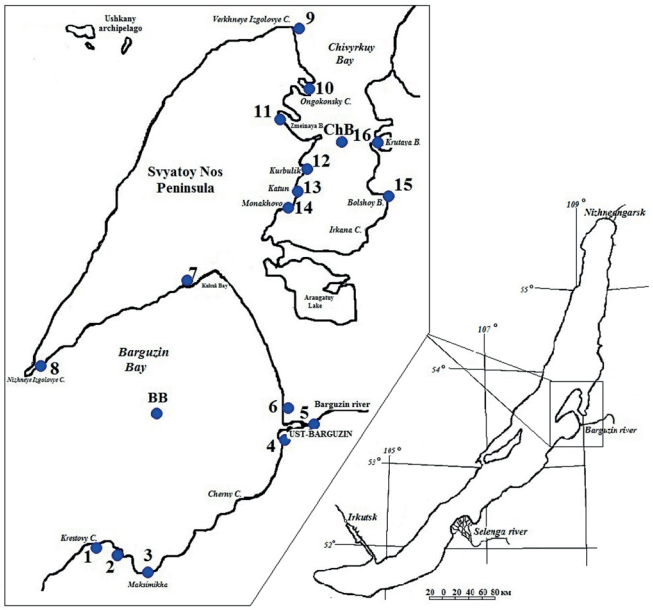

Fig. 1. Map of sampling stations in the Barguzin Bay and Chivyrkuy Bay, Lake Baikal.

3. Results and discussion

Barguzin Bay

On the coast of the Barguzin Bay, there are settlements Ust-Barguzin and Maksimikha, in 7 km from which the Rovesnik sports and recreation camp hosts over 500 people annually.

In the littoral zone of the Barguzin Bay, there are mostly sandy soils, and only on the coast of the Svyatoy Nos Peninsula, beaches are rocky. A feature of the northeastern part of the bay is the influx of the waters from the Barguzin River, which spread along the coasts of the bay (Tomberg et al., 2019). Agricultural production, including irrigation farming, is developed in the basin of the Barguzin River. The water temperature in the river during the study period was 20ºC. Water in the Barguzin River was enriched with silica, with a concentration of 3.8 mg/L. Among the mineral nitrogen compounds, there were nitrate ions in the concentration of 0.15 mg/L and nitrite ions in trace amounts; ammonium ions were not found. The concentration of mineral (phosphate) phosphorus in the water of the Barguzin River was 17 µg/L, and the total phosphorus – up to 41 µg/L (Fig. 2). COD was at the level of 10.6 mgO/L.

In the littoral zone of the Barguzin Bay, during the study period, the water temperature reached 22.5 ºC (station 2); near Krestovy Cape (station 1) at a depth of 5 m – 14.5 ºC. In the central part of the bay the temperature on the surface was 14.1 ºC, and in the near-bottom area, at a depth of 150 m,– 3.8 ºC.

The pH in the coastal waters ranged from 8.89 to 7.93 pH units, which indicates the intensive photosynthetic processes. In 7 km from the termination of the Kultuk Bay (station 7), the water edge zone is separated by a shingle spit and, hence, the water exchange is reduced, which affected the chemical composition of the water. Here, we recorded the minimum pH and low oxygen concentration (7.96 mg/L). In the centre of the bay, pH - 8,50 units, and the concentration of the dissolved oxygen was 9.6 mg/L.

The minimum concentration of the dissolved oxygen of 8.8 mg/L was observed at the station 4 (near the Barguzin River estuary), and the maximum concentration of 10.6 mg/L – in the water edge near

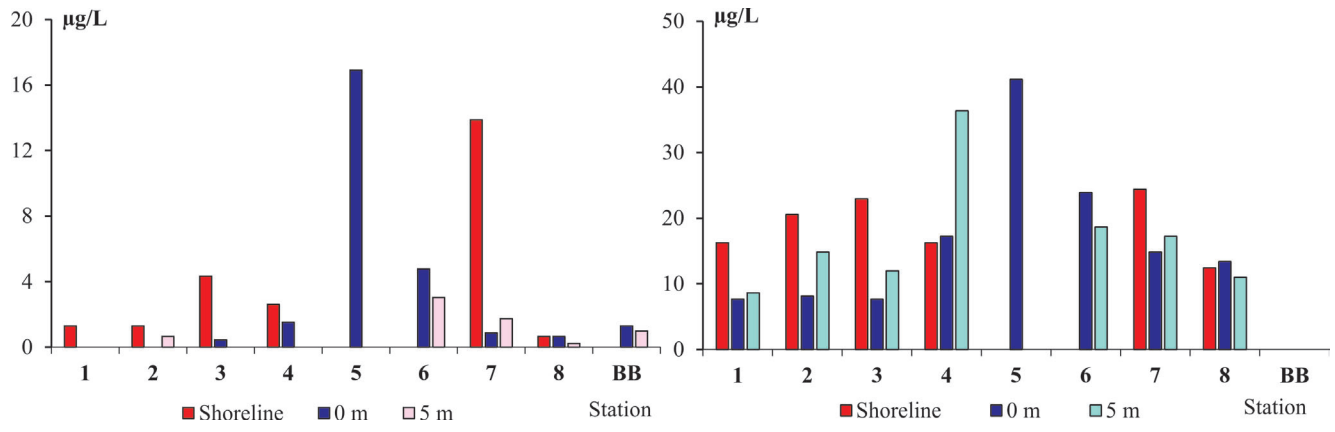

Fig. 2. Distribution of the concentrations of mineral (A) and total (B) phosphorus in the Barguzin Bay, August 2019.

the Rovesnik camp. Notably, the percentage of water saturation with oxygen at all stations was higher than 100%; the maximum water saturation was also recorded at the station near the camp.

The concentration of nutrients is the important indicator of the trophic state and quality of the coastal waters. Anthropogenic enrichment of waters with nutrients may lead to a radical restructuring of the aquatic ecosystem. The ion concentrations of ammonium and nitrites in the coastal waters of the Barguzin Bay was low (below 0.003 mg/L of nitrites and 0.01 mg/L of ammonium); nitrates were less than 0.10 mg/L. Phosphorus, the high concentration of which leads to eutrophication, affects strongly the productivity of water bodies. Measurements have shown that the amount of mineral phosphorus in the littoral zone does not exceed 5 μg/L. The concentration of the total phosphorus varies from 8 to 36 μg/L, and in the water edge zone, it is significantly greater than at a distance from the coast (Fig. 2). The maximum record of the total phosphorus was in the near-bottom area, in one km to the left of the Barguzin River estuary (station 4), which is associated with the influx of the river waters there. At station 7, the isolation of the water edge zone affected not only low oxygen concentration and pH but also an increase in the mineral phosphorus. In the centre of the bay, in the surface water layer, the concentration of mineral phosphorus was 1.3 μg/L.

The average concentration of silica in the bay was 0.7 mg/L; high concentration of up to 1.9 mg/L was observed at a one-km distance and to the right from the Barguzin River estuary, which is due to the influx of the river waters there, in which the silica concentration is 3.8 mg/L.

Chlorophyll *a* serves as a criterion in assessing phytoplankton biomass and its production, determining the quality of natural waters and the level of eutrophication of water bodies. The distribution of chlorophyll *a* in the coastal zone of the Barguzin Bay is uneven (Fig. 3). The water edge zone in the southern part of the bay (stations 1-3) is significantly distinguished by the amount of chlorophyll *a*. According to the previous studies (Tomberg et al., 2012; Timoshkin et al., 2016), there are large coastal accumulations of detritus in these areas, indicating an intensive development of phytobenthos in summer.

Chivyrkuy Bay

Chivyrkuy is the Baikal bay that runs the farthest inland; its length is approximately 25 km. The east and west coasts form a series of small and well-sheltered coves with a depth of approximately 5 m where the bottom of coasts and beaches are mostly sandy. On the west coast of the Chivyrkuy Bay, there are three main settlements: Katun, Kurbulik and Monakhovo. The bay places several hot springs, the most famous and visited of them is the Zmeiny spring on the west coast in the cove of the same name.

The coastal water of the Chivyrkuy Bay warms up well, and during the study period, the temperature in the littoral zone reached 20.5 ºC; in the centre of the bay, the water temperature was 18.6 ºC on the surface

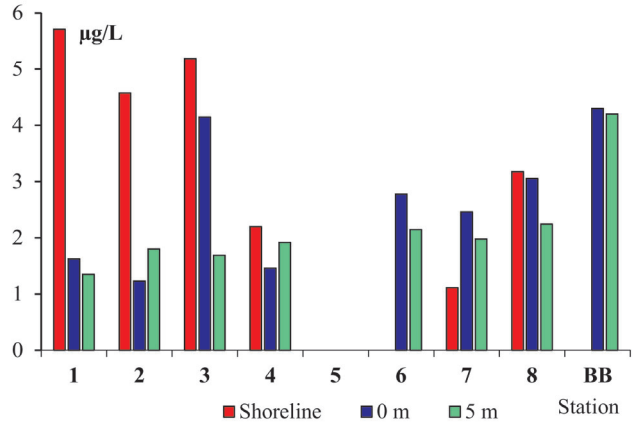

Fig. 3. Distribution of the chlorophyll *a* concentrations in the Barguzin Bay, August 2019.

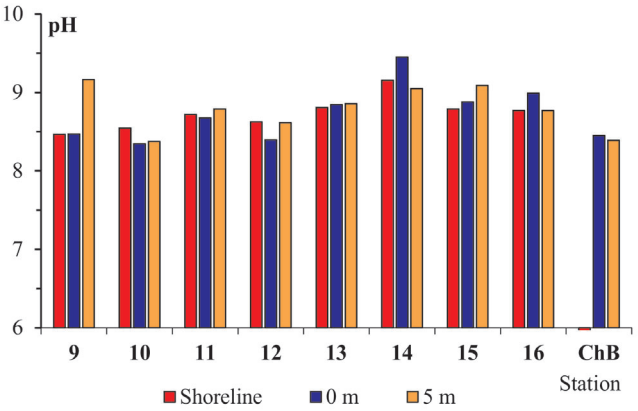

Fig. 4. Distribution of pH by stations in the Chivyrkuy Bay, August 2019.

and 14.6 ºC in the near-bottom area. It is worth noting that, unlike the Barguzin Bay, pH was higher there. The maximum pH - 9.45 was recorded at the bottom near the Monakhovo settlement (station 14) (Fig. 4), and the minimum (8.36 units)– in the centre of the Ongokon cove, and at the bottom, pH was 8.45 units.

The concentration of dissolved oxygen averaged 9.5 mg/L; the maximum value of 7.56 was recorded at the water edge near the Monakhovo settlement (station 14), and the average oxygen saturation of water was 140%.

In the coastal waters of the Chivyrkuy Bay, the concentration of the mineral phosphorus, like in the Barguzin Bay, generally, does not exceed 5 μg/L; high concentration of 21 μg P/L was only near the Monakhovo settlement (station 14) (Fig. 5A). The concentrations of the total phosphorus varied over a wide range from 11 to 182 μgP/L (Fig. 5B). Extremely high concentrations of the total phosphorus were in the Bolshaya cove (station 15), which is likely due to flooding of this area (coastal trees and bushes were flooded during sampling). In the Monakhovo settlement (station 14), high concentration of the total phosphorus is understandable: the coast is occupied by tourist tents without the appropriate infrastructure, there is also a large number of ships at the pier.

The average concentration of silica in the coastal waters of the Chivyrkuy Bay was 0.65 mg/L; an increase in its concentration of up to 0.9 mg/L was recorded

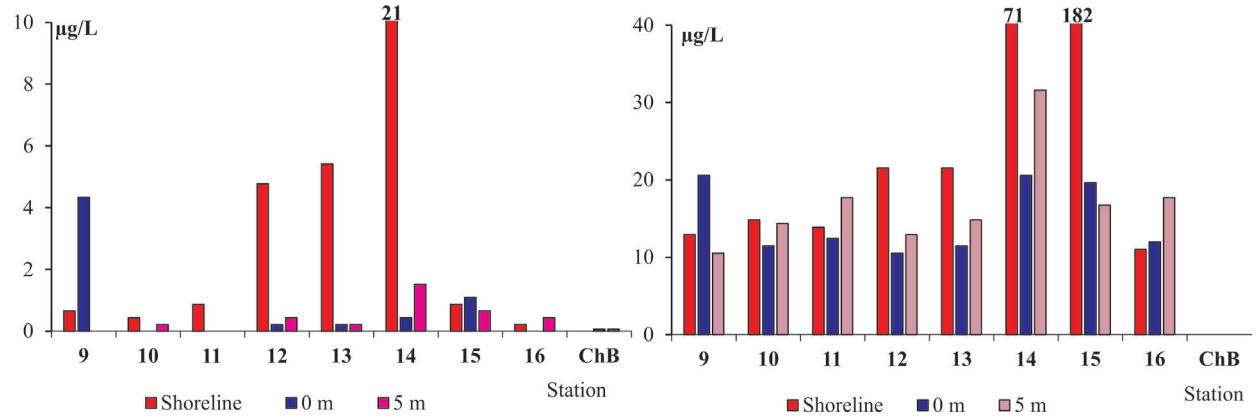

Fig. 5. Distribution of concentrations of mineral (A) and total (B) phosphorus by stations in the Chivyrkuy bay, August 2019.

in the Zmeinaya cove and the water edge of Ongokon cove (stations 10 and 11), which may be due to the influx of silica-rich groundwaters.

The concentrations of ammonium and nitrite ions both in the littoral zone and central part of the Chivyrkuy Bay were below the detection limits of the applied research methods. High ammonium ion concentrations of up to 0.010 and 0.29 mg/L with high oxygen concentration in the Monakhovo settlement indicate the faecal pollution of waters. The amount of nitrate ions in the coastal waters of the Chvyrkuy Bay, generally, does not exceed 0.1 mg/L. Their maximum amount of 0.53 mg/L was recorded in the water edge near the Kurbulik settlement (station 12), which is most likely due to the proximity of the settlement with no sewage system. The influx of nutrients and organic substances from tourist campsites in the Monakhovo settlement and a sufficient warming up of the water causes the intensification of the development of algae, as evidenced by the high concentration of chlorophyll *a* in the water edge and COD values (Fig 6A, 6B). Notably, at this station, primary production was 1.86 mg/L. This is the maximum value obtained during our studies, whereas the average value of the primary production in the Chivyrkuy Bay was 0.19 mg/L.

The nutrient concentrations at some stations of the littoral zone in the Chivyrkuy Bay were higher than in the background areas. It should be noted that previous studies (Tomberg et al., 2012; Vorobyovskaya et al., 2016; O'Donnell et al., 2017) showed the same problem areas, indicating the constant pollution of the coastal waters in the bay.

Assessment of water quality in the bays

Many methods determine the quality of water in water bodies and watercourses based on chemical indicators. The maximum permissible concentration (MPC) is mostly used to assess the water quality according to sanitation and hygiene standards (hygiene standard GN 2.1.5.1315-03, 2003; hygiene standard GN 2.1.5.2280-07, 2007; sanitary rules and norms SanPiN 2.1.5.980-00, 2000), standards for fishery use of water bodies (Prikaz Rosrybolovstva, 2010), the environmental and sanitation indicators (Oksiyuk et al., 1993) and comprehensive water pollution index (CWPI) (regulatory guide RD 52.24.643-2002, 2003). Comprehensive indicators of water quality provide a unified assessment and comparison of water purity at different sites and at different times as well as detection of substances that mainly contribute to the overall water pollution.

Among the entire set of the studied elements, hygiene standard GN 2.1.5.1315-03 (2003) normalizes mineral forms of nitrogen as well as phosphates. We identified no excess of MPCs for these elements in the waters of the bays. According to the standards for fishery use of water bodies, we also did not identify the excess of MPCs for the studied elements. Sanitary rules and norms SanPiN 2.1.5.980-00 normalize pH, BOD5 and COD. We recorded the excess of the pH standard for drinking and domestic water supply as well as for recreational water use in 19 of 24 water samples from the Chivyrkuy Bay and in 5 of 20 water samples from the Barguzin Bay.

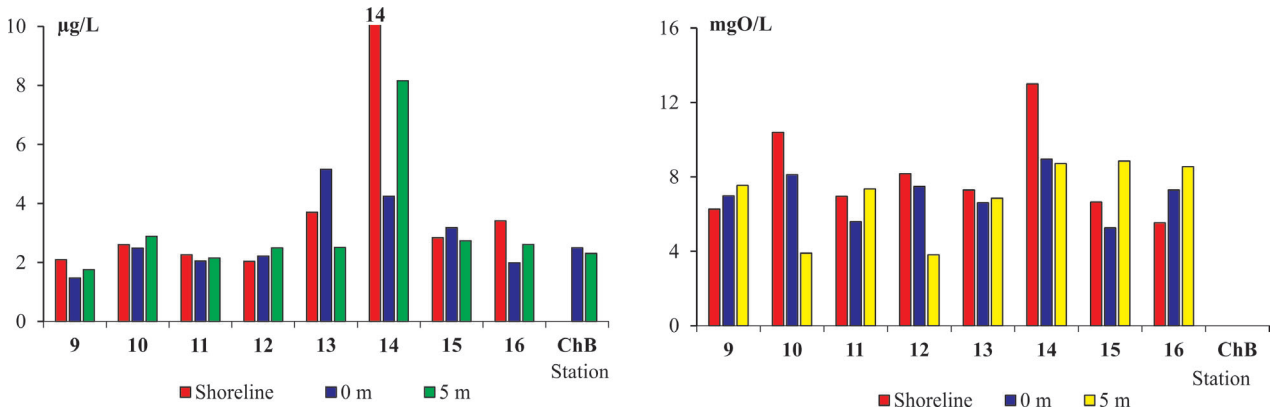

Fig. 6. Distribution of the chlorophyll *a* concentrations (A) and COD (B) by stations in the Chivyrkuy Bay, August 2019.

According to **environmental and sanitation classification** (Oksiyuk et al., 1993), the waters of the bays can be assessed as polluted to a different degree based on pH and oxygen saturation of water. The lower water quality is in the Chivyrkuy Bay (Fig. 7). This is due to a large number of organized and independent tourists, lack of sewage systems and discharge of domestic and waste waters from the ships near the coast. A large amount of dissolved oxygen in the water can also have a polluting effect on the water body. However, the phytoplankton development may cause high oxygen concentration in the water due to the difference in rates of oxygen removal into the atmosphere (evasion) and intensity of water saturation with oxygen resulted from photosynthesis. Indeed, a low concentration of carbon dioxide (more than 8 pH units), compounds of nitrogen and phosphorus as well as high chlorophyll *a* concentration (14.4 μg/L near the Monakhovo settlement) indicate the active photosynthesis in the bays, an increase in the biomass of not only phytoplankton but also phytobenthos (fouling on stones) and higher aquatic vegetation. The biomass decomposition of all algae at the end of the growth of aquatic vegetation, as well as the isolation behind the ice cover from the atmosphere, will lead to an increase in organic substances and nutrients, a decrease in oxygen and overall deterioration of water quality, which can result in disturbance of trophic links and overall degradation of the ecosystem.

To calculate CWPI, we used the data on the concentrations of mineral forms of nitrogen, mineral phosphorus, COD, pH, and oxygen saturation of water. The CWPI calculation has revealed that based on the occurrence frequency the water pollution in the Barguzin Bay is “unstable” according to the pH value and “typical” according to the oxygen saturation of water.

Based on the frequency of the MPC excess, the level of water pollution in the Barguzin and Chivyrkuy bays is “low” according to both the pH value and the oxygen saturation of water.

In general, based on CWPI, the water in the Barguzin bay belongs to the first contamination class, conditionally pure, and the water in the Chivyrkuy Bay belongs to the second contamination class, conditionally polluted.

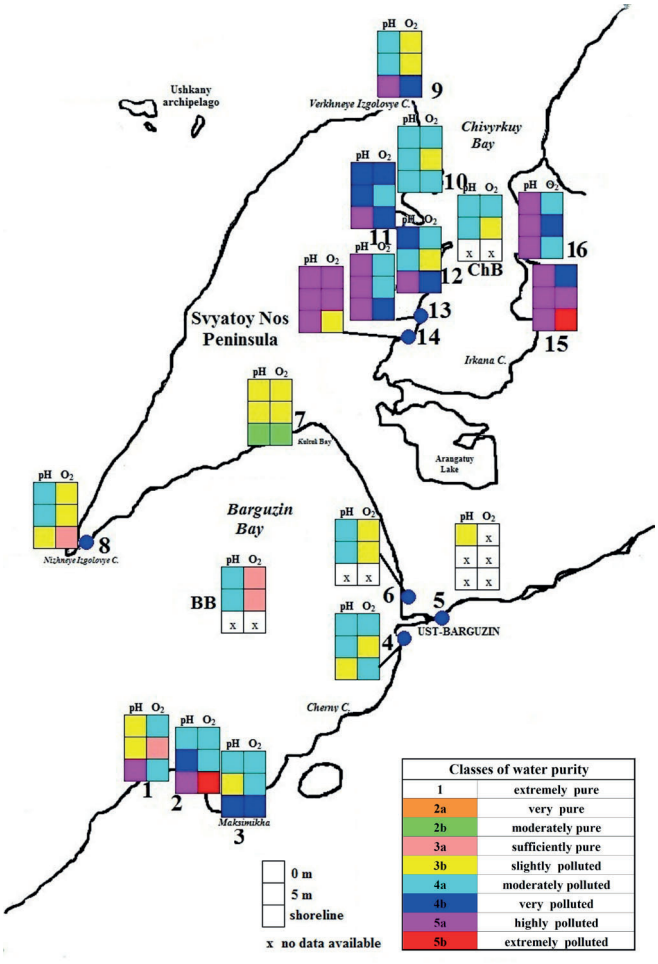

Fig. 7. Assessment of the quality of waters in the Chivyrkuy and Barguzin bays according to environmental and sanitation indicators in the summer of 2019. Colours indicate the class of water quality (Oksiyuk et al., 1993) based on pH (first column) and percentage of the oxygen saturation of water (second column).

4. Conclusions

Based on our measurements, the assessment of the quality of the waters in the bays during summer revealed no excess of MPCs according to sanitation and hygiene standards and standards for fishery use of water bodies. According to environmental and sanitation classification, the waters in the bays are assessed as polluted to a different degree, with the lower water quality in the Chivyrkuy Bay.

According to CWPI, the waters in the Chivyrkuy and Barguzin bays are assessed as conditionally polluted and conditionally pure, respectively. At the same time, we assume that upon the completion of the grown of the aquatic vegetation, pH and oxygen saturation of water will decrease, and the water quality will improve according to these indicators. Nevertheless, the decomposition of dead algae will lead to an increase in the number of nutrients and organic matter, which, in turn, will deteriorate the water quality already according to these indicators.

To improve the environmental state of the Barguzin and Chivyrkuy Bays of Lake Baikal, it is necessary to fulfil water protection measures aimed at reducing anthropogenic impact by reducing recreational and domestic pressure, constructing tourist infrastructure for existing campsites and organizing wastewater treatment systems for ships.

Acknowledgements

This study was carried out within the framework of State Tasks Nos. 0345-2020-0008 and AAAA-A17-117021310142-5 and with the partial support of Russian Foundation for Basic Research and the Government of the Republic of Buryatia of the Russian Federation (Grant No. 18-45-030007)

References

Federal environmental regulation PND F 14.1:2:4.154-99. 2012. Quantitative chemical analysis of water. The method for measuring permanganate oxidation in samples of drinking, natural and waste waters by the titrimetric analysis. Moscow: Federal Service for the Supervision of Natural Resources. (in Russian)

Federal environmental regulation PND F 14.1:2:4.190-03. 2007. Quantitative chemical analysis of water. Method for determination of dichromate oxidation (chemical oxygen demand) in samples of natural, drinking and waste waters by the photometric method using the Fluorat-02 liquid analyser. Moscow: Ministry of Natural Resources of the Russian Federation. (in Russian)

Hygiene standard GN 2.1.5.1315-03. 2003. The maximum permissible concentrations (MPCs) of chemicals in the water of water bodies of domestic, drinking, and cultural and domestic water use, as amended on July 13, 2017. Moscow: Ministry of Health of the Russian Federation. Russian Register of Potentially Hazardous Chemical and Biological Substances of the Ministry of Health of Russia. (in Russian)

Hygiene standard GN 2.1.5.2280-07. 2007. The maximum permissible concentrations (MPCs) of chemicals in the water of water bodies of domestic, drinking, and cultural and domestic water use. Amendments No. 1 to GN 2.1.5.1315-03. Bulletin of regulatory acts of federal executive bodies No. 50. (in Russian)

Kravtsova L.S., Izhboldina L.A., Khanaev I.V. et al. 2012. Disturbances of the vertical zoning of green algae in the coastal part of the Listvennichnyi Gulf of Lake Baikal. Doklady Biological Sciences 448: 227-229. DOI: 10.1134/S0012496612060026

Kravtsova L.S., Izhboldina L.A., Khanaev I.V. et al. 2014. Nearshore benthic blooms of filamentous green algae in Lake Baikal. Great Lakes Research 40: 441-448. DOI: 10.1016/j.jglr.2014.02.019

National Standard GOST 17.1.4.02-90. 2010. Water. Method of spectrophotometric determination of chlorophyll *a*. Moscow: Standartinform. (in Russian)

National standard GOST 18309-2014. 2015. Water. Methods for the determination of phosphorus-containing substances. Moscow: Standartinform. (in Russian)

National standard GOST 33045-2014. 2019. Water. Methods for the determination of nitrogen-containing substances. Moscow: Standartinform. (in Russian)

O'Donnell D.R., Wilburn P., Silow E.A. et al. 2017. Nitrogen and phosphorus colimitation of phytoplankton in Lake Baikal: insights from a spatial survey and nutrient enrichment experiments. Limnology and Oceanography 62: 1383-1392. DOI: 10.1002/lno.10505

Oksiyuk O.P. Zhukinsky L.P., Braginsky et al. 1993. A comprehensive environmental assessment of the quality of surface waters. Gidrobiologicheskij Zhurnal [Hydrobiological Journal] 29: 62-72. (in Russian)

Prikaz Rosrybolovstva № 20. 2010. "On the approval of water quality standards for water bodies used for fishery, including standards for maximal allowable concentrations of hazardous substances in water of water bodies used for fishery". (in Russian)

Regulatory guide RD 52.24.383-2018. 2018. Mass concentration of ammonia nitrogen in the water. Measurement technique by the photometric method in the form of indophenol blue Rostov-on-Don: Rosgydromet. (in Russian)

Regulatory guide RD 52.24.419-2005. 2004. Mass concentration of dissolved oxygen in water. Measurement technique by iodometry. Rostov-on-Don: Rosgydromet. (in Russian)

Regulatory guide RD 52.24.420-2006. 2006. Biochemical oxygen demand. Measurement technique by light and dark bottle method. Rostov-on-Don: Rosgydromet. (in Russian)

Regulatory guide RD 52.24.433-2005. 2005. Mass concentration of silica in the surface waters. Measurement technique by the photometric method in a yellow form of molybdosilicic acid. Rostov-on-Don: Rosgydromet. (in Russian)

Regulatory guide RD 52.24.495-2017. 2017. Hydrogen indicator of waters. Measurement technique by potentiometric method. Rostov-on-Don: Rosgydromet. (in Russian)

Regulatory guide RD 52.24.643-2002. 2003. Methodological guidelines. A method for a comprehensive assessment of the degree of pollution of surface waters by the hydrochemical indicators. St. Petersburg: Gidrometeoizdat. (in Russian)

Rukovodstvo po metodam gidrobiologicheskogo analiza poverkhnostnykh vod i donnykh otlozheniy [Guide to methods for hydrobiological analysis of surface water and bottom sediments]. 1983. In: Abakumov V.A. (Ed.). Leningrad: Gydrometeoizdat. (in Russian)

Sanitary rules and norms SanPiN 2.1.5.980-00. 2000. Hygienic requirements for surface water protection. Moscow: Federal Centre for State Sanitary and Epidemiological Supervision of the Ministry of Health of Russia. (in Russian)

Timoshkin O.A., Samsonov D.P., Yamamuro M. et al. 2016. Rapid ecological change in the coastal zone of Lake Baikal (East Siberia): is the site of the world's greatest freshwater biodiversity in danger? Journal of Great Lakes Research 42: 487-497. DOI: 10.1016/j.jglr.2016.02.011

Tomberg I.V., Sakirko M.V., Domysheva V.M. et al. 2012. First data on the chemical composition of interstitial waters of the splash zone of Lake Baikal. Izvestiya Irkutskogo Gosudarstvennogo Universiteta. Seriya "Biologiya. Ekologiya" [The Bulletin of Irkutsk State University. Series "Biology. Ecology"] 5: 64-74. (in Russian)

Tomberg I.V., Sinyukovich V.N., Ivanov V.G. et al. 2019. Transformation of the chemical composition of waters from the Barguzin River in the Barguzin Bay (Lake Baikal). Limnology and Freshwater Biology 4: 275-280. DOI: 10.31951/2658-3518-2019-A-4-275

Vorobyovskaya E.L., Gorshkova O.M., Ermolychev F.B. et al. 2016. The study of water pollution in the Chivyrkuy Bay of the Trans-Baikal National Park in the winter of 2016. In; International Scientific and Practical Conference «Education and Science in the XXI Century», pp. 133-137.

Limnology and Freshwater Biology 2020 (2): 397-404 DOI:10.31951/2658-3518-2020-A-2-397

Original Article

ISSN 2658-3518
LIMNOLOGY FRESHWATER BIOLOGY
www.limnolfwbiol.com

Assessment of water pollution near the deep oil seep in Lake Baikal

Gorshkov A.G., Izosimova O.N.*, Pavlova O.N., Khlystov O.M., Zemskaya T.I.

Limnological Institute, Siberian Branch of the Russian Academy of Sciences, Ulan-Batorskaya Str., 3, Irkutsk, 664033, Russia

ABSTRACT. Water purity was assessed at the site of a deep oil seepage near Cape Gorevoy Utes (Central Baikal). Polycyclic aromatic hydrocarbons (PAHs) and *n*-alkanes were determined in different types of oil-containing samples collected at this section of Lake Baikal. The set of studied samples included: (i) samples of water from the surface water layer; (ii) samples of water from different depths; (iii) oil on the water surface; (iv) oil from a sediment core. In the surface water layer and the water column, the total concentration of *n*-alkanes ranged from 0.2 to 5.3 μg/L and did not exceed the 0.1 maximum permissible concentration (MPC_{fish} = 50 μg/L) established for hydrocarbons in water bodies of fishery importance. PAHs with carcinogenic properties were less than 0.1 ng/L. The total concentration of PAHs found in the water column did not exceed 110 ng/L; toxic equivalent (TEQ) values ranged from 0.001 to 0.110 ng/L. The distribution of petroleum hydrocarbons from the seepage site was limited, and water pollution was localised. The low level of water pollution is associated with natural mechanisms in the Baikal ecosystem. Microbiological community and phytoplankton make a decisive contribution to the purity of Baikal water, and oil fractionation during deep discharge contributes to the bioavailability of petroleum hydrocarbons.

Keywords: Oil seeps Contamination of water Lake Baikal

1. Introduction

Natural oil seepage in freshwater lakes is associated with rift zones: Lake Tanganyika – with the East African Rift (Simoneit et al., 2000), Lake Chapala – with the Citala Rift (E-W) (Zarate-del Valle et al., 2006), and Lake Baikal – with the Baikal rift. High heat flux in the rift zone of Baikal (76 mW/m^2 on average, Golmshtok et al., 2000) contributes to the heating of sedimentary formations and stimulates the generation of hydrocarbons. According to data on seismic studies, oil and gas may accumulate in the structure of the Cenozoic sedimentary basins in Baikal, with a potential resource of 500 million tons (Kontorovich et al., 2007). The presence of oil is evidenced by natural oil seepage in the form of asphalt that appears along coastal cliffs or comes from depths of 10–15 m to the water surface of the lake approximately 300–500 m from the shore, forming oil slicks from the emerging tar balls with a diameter of up to 1.5 m. In wintertime, oil accumulates under the ice, filling fractures in the ice cover. Examination of this oil indicates that it is an aromatic-naphthenic type, in which there are no normal alkanes, monomethyl alkanes or acyclic isoprenoids. The flow of petroleum hydrocarbons from the bottom of the lake is 0.1–5 tons of heavy oil per year (Kontorovich et al., 2007).

In 2005, a new deep oil seepage was discovered near Cape Gorevoy Utes (Central Baikal). At this site, there were numerous oil slicks with a diameter of up to 1 m. The oil collected at the time of its emergence on the water surface had an extremely high concentration of *n*-alkanes and was identified as non-biodegraded paraffin oil. The oil sampled from the water surface contained a full range of petroleum hydrocarbons: *n*-alkanes, *i*-alkanes, alkyl-cyclohexanes, isoprenoids (pristane and phytane), PAHs and hopanes as well as a complex of unique molecular biomarkers (Gorshkov et al., 2006; Kashirtsev et al., 2006; Khlystov et al., 2007; Kontorovich et al., 2007). In 2008, investigations of the bottom sites near the oil seepage using the MIR deep-sea manned submersibles at depths of 870–920 m revealed structures consisting of paraffin petroleum asphalt, through which oil discharged. At sites with a flat bottom and near these structures, there were accumulations of liquid oil droplets that floated without any periodicity (Khlystov et al., 2009).

According to estimates (Khlystov et al., 2007; Kontorovich et al., 2007), the amount of oil entering Baikal waters at this site does not exceed 4 t/y, which is not comparable to the volumes of industrial oil discharged into the surface waters of the world's oceans during technological disasters (Hazen et al., 2010; Vila

*Corresponding author.
E-mail address: smileoc@mail.ru (O.N. Izosimova)

et al., 2010; Yender and Stanzel, 2011). Nevertheless, constant oil emission, low water temperature and the long replacement period of lake water by tributaries (ca. 330 years) increase the environmental risk of a decline in Baikal water quality. It is also worth noting that natural oil seeps are dynamic systems that develop over time and are characterized by the unpredictability of the emergence of new seeps in time and space.

Lake Baikal is the globally important drinking water source containing 20% of the world's surface freshwater. To assess the purity of water in the area of deep oil seepage near Cape Gorevoy Utes, a natural source of oil hydrocarbons, samples of freshly emitted oil and oil slicks from the water surface as well as the water samples from various layers in the water column were collected. A bottom sediment core was also sampled in the area of deep oil seepage. In all samples of oil, water, and bottom sediments, *n*-alkanes and PAHs were studied. *n*-Alkanes are the dominant components of oil entering the lake in this area. PAHs are a minor component of oil, but this class of substances is among the priority pollutants and subject to constant monitoring in the environment.

2. Materials and methods

Investigations were carried out in 2016 and 2019 at the site of the natural oil seepage near Cape Gorevoy Utes (10 km from the coast, 900 m depth, Central Baikal; coordinates 53°18'33''N 108°23'46'' E). Oil, water from the surface and deep layers, and bottom sediments were sampled on board the research vessel "G. Yu. Vereshchagin" at seven stations, R4 - R10 (Fig. 1). Stations R4, R5, R7 - R10 were located at sites with oil slicks on the surface; station R6 was at a site without oil slicks. Oil slicks were sampled using a sterile beaker and poured into 1 L glass bottles. Water samples were taken using an SBE 32 Carousel Water Sampler from depths of 0, 5, 200, 400, 600, 800, and 860 m and poured into 1 L glass bottles. Fifty mL of dichloromethane was added to each water sample; then the mixture was shaken, covered with a lid with aluminium foil and stored at +5 °C until analysis.

The bottom sediment core was sampled at the VER-16-01 (GC4) station using a gravity corer with a plastic liner. The upper part of the core (from the surface down to 140 cm) contained gas-saturated aleuropelitic muds impregnated with oil; the lower part (from 140 to 310 cm) was clay, in which there were vertical or inclined discharge channels with diameters of up to 5 mm, split and degasification cracks of 1–2 mm, and horizontal aleuro-sandy interlayers also impregnated with oil.

Normal hydrocarbons and PAHs in water samples were determined by liquid-liquid extraction with dichloromethane. Before extraction, 100 μL of PAH solution (a mixture of naphthalene-d_8, acenaphthene-d_{10}, phenanthrene-d_{10}, chrysene-d_{12}, and perylene-d_{12}) in acetonitrile with a concentration of 5 ng/μL for each polyarene; 200 μL squalane solution in dichloromethane with a concentration of 330 ng/μL; and 25 mL dichloromethane were added to the water samples. The mixture was shaken for 3 min and moved to a 1 L separatory funnel. After phase separation, the lower dichloromethane layer was separated, and the extraction was repeated with a new 25 mL portion of extractant. The extracts were mixed and concentrated to a volume of ~1 mL. Na_2SO_4 (calcined and chemically

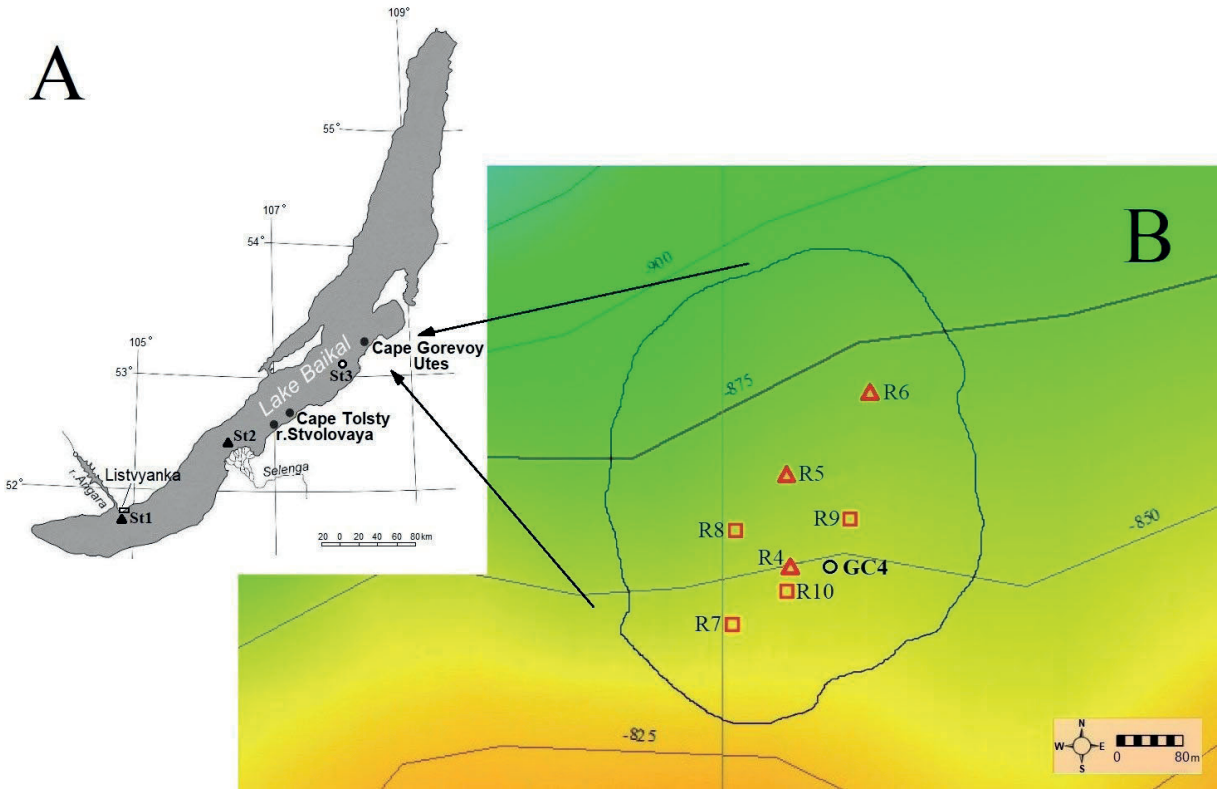

Fig. 1. Map of Lake Baikal: A - ● - sites of oil seeps; ○,▲ – reference stations; B - △, □ - sampling stations.

pure) was added to the concentrate, and the mixture was shaken and centrifuged. The supernatant was transferred to the autosampler vials of the gas chromatography-mass spectrometer. The extracts of water samples containing oil (after chromatography analysis) were dried to constant weight; the resulting residue was weighed. The content of *n*-alkanes and PAHs in these samples was calculated relative to the amount of recovered oil.

To determine *n*-alkanes and PAHs in the bottom sediment core, samples that differed in maximum oil content were taken. The samples were dried at room temperature to constant weight and then homogenised. Two samples (2–3 g) were taken, to which internal standards of 25 μL PAH solution and 50 μL squalane solution were added. PAHs and *n*-alkanes were twice extracted with 15 mL of dichloromethane in an ultrasonic bath, each time for 20 min. The extracts were mixed and centrifuged. The supernatant was taken and concentrated to a volume of ~1 mL; concentrate then was diluted with *n*-hexane in the ratio of methylene chloride: *n*-hexane = 1:10 (v/v); the mixture was kept at +5 °C for 24 h, the sample was centrifuged, and the supernatant was transferred to the flask of the chromatography autosampler and concentrated under an argon flow to a volume of ~ 0.1 mL. The extracts of bottom sediment samples containing oil were dried to constant weight; the resulting residue was weighed. The content of *n*-alkanes and PAHs in these samples was calculated relative to the amount of recovered oil.

In the collected samples, *n*-alkanes and PAHs were determined: *n*-alkanes as homologous series from C_8 to C_{30} and 24 PAH compounds, including 16 priority polyarenes: naphthalene (Nap); 1-methylnaphthalene (1mNa); 2-methylnaphthalene (2mNa); acenaphthylene (Acy); acenaphthene (Ace); fluorene (Fl); phenanthrene (Ph); anthracene (An); 1-metylphenanthrene (1mPh); 2-metylphenanthrene (2mPh); 3-metylphenanthrene (3mPh); 9-metylphenanthrene (9mPh); fluoranthene (Flu); pyrene (Pyr); benzo[a]anthracene (BaA); chrysene (Chr); benzo[b]fluoranthene (BbF); benzo[k] fluoranthene (BkF); benzo[e]pyrene (BeP); benzo[a] pyrene (BaP); perylene (Per); indeno[1,2,3-cd]pyrene (InP); benzo[g,h,i]perylene (BghiP); and dibenzo[a,h] anthracene (DahA).

PAHs and *n*-alkanes in the samples were determined using an Agilent Technologies 7890B GC System 7000C GC-MS Triple Quadrupole Gas Chromatography-mass spectrometer with an OPTIMA® 17 MS capillary column (30 m × 0.25 mm × 0.25 μm). The GC operating parameters were from 50 to 310 °C at a heating rate of 20 °/min, then maintaining the column at the final stage at 310 °C for 35 min. The temperatures of the injector and ion source were 290 °C and 250 °C, respectively; the volume of the injected sample was 2 μL without flow splitting, and the electron impact ionization energy was 70 eV. The chromatograms of sample extracts were recorded in the SCAN mode by scan mass spectrum from 50 to 600 m/z. Peaks were identified using the LIB2NIST v.1.0.0.8 mass spectral data conversion program for 150,000 compounds. For quantification of *n*-alkanes and PAHs, chromatograms of samples were recorded in the SIM mode: the peaks of *n*-alkanes with 57 and 71 m/z; the peaks of PAHs with 128, 136, 142, 152, 154, 164, 166, 178, 188, 192, 202, 228, 240, 252, 264, 276, and 278 m/z. The peaks were identified by relative retention times.

Quantification was performed using the internal standard method. The chromatograph was calibrated in the range of the expected PAH and *n*-alkane concentrations in the extracts with the preparation of solutions of PAHs and *n*-alkanes with a concentration of 0.05-50 ng/mL. The calibration solutions were prepared by diluting the certified PAH and *n*-alkane mixture (Supelco, USA) with an *n*-hexane–acetone mixture (1:1, v/v). The concentration of analytes in the samples was calculated as the average value of the results of two determinations in one sample. The PAH and *n*-alkane extraction efficiency were approximately 70% - 80%. Limit of detection (LOD) was calculated as the threefold standard deviation peak area of the PAH and *n*-alkane levels in procedure blanks, in the water: PAH - 0.1-1.0 ng/L, *n*-alkane – 2 ng/L; in the oil: PAH - 1-10 ng/g, *n*-alkane – 100 ng/g. Relative standard deviation (RSDs) for determining PAHs and *n*-alkanes was estimated within a range from 15% to 20% for individual analytes.

Toxic equivalents (TEQ) were calculated according to the following equation:

$$TEQ = C_i \times TEF_i,$$

where C_i is PAH concentration in ng/L, and TEF_i are the toxicity coefficients for individual PAHs relative to BaP. The following TEFs were used for PAHs from Baikal waters: 0.001 for Na, Acy, Ace, Fl, Ph, Flu, and Pyr; 0.01 for An and Chr; and 0.1 for BbF (Nisbet and LaGoy, 1992).

3. Results and discussion

3.1. *n*-Alkanes and PAHs in oil on the water surface and bottom sediments

n-Alkanes, isoprenoids (pristane and phytane) and PAHs were identified in the composition of freshly emitted oil on the water surface. Moreover, *n*-alkanes were the dominant component in the oil. In the oil slicks, total concentrations of *n*-alkanes (Σ_{alk}) and PAHs (Σ_{PAH}) were low, up to four times lower than in freshly emitted oil (Table 1). In the slicks, *n*-alkanes are represented by homologous series C_{12} - C_{26}. The ratio of light and heavy homologues in this series ($R_{alk} = \Sigma[C_8 – C_{18}]/\Sigma[C_{19} – C_{29}] \geq 0.7$) indicated a partial loss of the light fraction. Records of an unresolved complex mixture (UCM) of branched and cyclic hydrocarbons on chromatograms of slick samples and a decrease in naphthalenes in the PAH fraction confirmed oil deformation on the surface of the lake resulting from evaporation and weathering. PAHs detected in oil on the water surface included 20 compounds. PAH ratios, An/(An + Ph) and Flu/(Flu + Pyr), indicated a petrogenic source of oil (Yunker et al., 2002), and ratios of isoprenoids (pristane/phytane) in oil slicks corresponded to those in the freshly emitted oil.

Table 1. Features of the oil on the water surface

Feature	Freshly emitted oil on the water surface	Oil slicks on the water surface
Homologous series of *n*-alkanes	C_8-C_{29}	C_{13}-C_{26}
Σ_{alk}, %	90	21-24
$R_{alk} = \Sigma[C_8\text{-}C_{18}]/\Sigma[C_{19}\text{-}C_{29}]$	1.0	0.7-0.9
The Pr/Ph ratio	6.7	6.1-6.8
Σ_{PAH}, ppm	1500	530-650
Σ_{naph}, % of total PAHs	32	5.0-25
BaP number, ppm	3.7	5.1-5.6
The An/(An + Ph) ratio	0.09	0.04
The Flu/(Flu + Pyr) ratio	0.34	0.28-0.33

Station R6 (Fig. 1) differed by the lack of surface oil slicks. Nevertheless, *n*-alkanes (C_{12} - C_{26}) and PAHs (14 compounds) were found in surface water samples (Table 2). High molecular weight homologues dominated in the fraction of *n*-alkanes (Σ_{alk} 0.2 – 5.3 μg/L; R_{alk} = 0.7). In the composition of PAHs, unlike that of oil films, there were no high molecular weight PAHs: the content of Per, InP, BghiP, and DahA were below the limit of their quantification (0.1 ng/L); the total concentration of naphthalenes (Σ_{naph}) corresponded to a range from 4.1 to 32 ng/L (30% - 63% of Σ_{PAH}).

In the fractures and interlayers of the bottom sediment core, the amount of oil was minimal, up to 2.9% of the core mass, and the Σ_{alk} concentration varied from 0.10 to 1.4% (Table 3). In the oil from upper layers of the core (samples from 0.40 and 50 cm layers) high molecular weight paraffins dominated, apparently resulting from the migration of the light fraction to the lake water. The oil composition in the core sample from a deep layer (274 cm) showed an equal ratio of light and high molecular homologues of *n*-alkanes (a series from C_{13} to C_{29}). PAHs identified in the oil from the core contained 24 compounds (Σ_{PAH} 400-1400 ppm), including high molecular weight polyarenes at a level of $^<$ 0.1–10 ppm. The amount of BaP in the core samples did not exceed 3.2–9.8 ppm. The PAH composition and ratio of indicator polyarenes corresponded to those in the freshly emitted oil on the water surface.

3.2. *n*-Alkanes and PAHs in the water column

In the water column (5–860 m at stations R4, R5, R7 – R10), normal hydrocarbons are identified as homologous series from C_{12} to C_{27}, with the Σ_{alk} concentration ranging from 0.2 to 4.5 μg/L (Table 2). The average value Σ_{alk} concentration is 1.6 μg/L, and 1.5 times higher than the median value, indicating a heterogeneous distribution of alkanes in the water column. At station R6 (station distinguished by the lack of surface oil slicks), the Σ_{alk} content in water samples from the 5–860 m layer corresponded to a narrow range of values, from 0.2 to 0.9 μg/L; low molecular weight homologues dominated most of the samples. At station R4, layers of 200, 600, and 800 m had a significant content of high homologues (Fig. 2).

The PAH fraction in the water column (5–800 m layer at stations R4 – R10) had a narrow series of low molecular weight polyarenes, including Na, Ace, Fl, Ph, Flu, and Pyr. In single samples, there were Acy, Chr, BbF, and BeP. The total number of naphthalenes (Σ_{naph}) had a maximum proportion (up to 85%) in the total Σ_{PAH} concentration, which was within the range from 1.0 to 110 ng/L (Table 2). At station R6, the content of PAHs in water samples differed in a narrow range of detected concentrations, from 3.9 to 15 ng/L.

It is worth noting that extreme concentrations of *n*-alkanes and PAHs were detected in the water sample from the 200 m layer at station R4, in which the Σ_{alk} concentration reached 330 μg/L, and Σ_{PAH} concentration reached 100 ng/L. Normal hydrocarbons were represented by a series from C_{13} to C_{29}, with a dominance of high molecular weight homologues, similar to the *n*-alkane content in samples from the upper layers of the core. The PAH concentration in this sample was also higher than in the samples from other layers of the water column (by an order of magnitude), and the content of naphthalenes in the fraction was estimated at the maximum level, up to 85% of the Σ_{PAH} concentration.

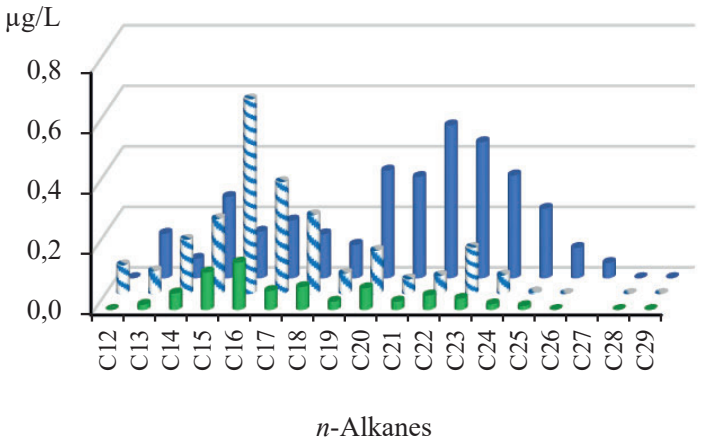

Fig. 2. A ratio of homologues of n-alkanes in water extracts from the 600 m layer:
- station R4; Σalk = 3.4 μg/L; Ralk = 0.4;
- station R5 (Σalk = 2.4 μg/L; Ralk = 3.5.
- station R6 (Σalk = 0.73 μg/L; Ralk = 2.0

Table 2. Content of *n*-alkanes and PAHs in the water column in 2016 and 2019

Feature	Water layer, m						
	0	5	200	400	600	800	860
	Stations R6						
Σ_{alk}, μg l^{-1}	0.2 – 5.3	0.7	0.2 - 0.7	0.7	0.2 - 0.7	0.3 - 0.9	0.2 - 0.4
R_{alk}	0.7 – 0.8	3.3	1.7 - 2.9	2.1	0.7 - 2.0	1.4 - 3.0	1.0 - 4.3
Σ_{PAH}, ng l^{-1}	14 - 51	5.4	4.7	10	15	14	3.9
$\Sigma_{naph.}$, ng l^{-1}	4.1 - 32	3.1	3.0	9.0	5.0	4.1	3.1
R_{PAH}^{**}	0.6	0.7	1.0	0.7	0.6	0.6	0.7
Feature	**Stations R4, R5, R7 – R10**						
Σ_{alk}, μg l^{-1}	-	1.3 - 4.5	0.2 – 2.8 (330*)	0.8 - 4.0	0.2 -3.4	0.3 - 2.6	0.2 – 3.7
R_{alk}^{1}	-	1.3 - 2.1	0.6 – 1.2	0.9 - 1.7	0.4 -3.2	0.6 – 5.8	1.0 – 3.2
Σ_{PAH}, ng l^{-1}	-	18 - 90	18 – 100	14 – 59	7.2 – 62	5.2 - 47	12 – 110
$\Sigma_{naph.}$, ng l^{-1}	-	5.7 – 67	13 -87	3.2 - 7.9	5.1 -54	3.3 – 32	6.2 – 83
R_{PAH}^{**}	-	0.6	0.6	0.6	0.5	0.6	0.6

Note: * – the extreme concentration of *n*-alkanes; ** – the ratio of the Flu/(Flu + Pyr) concentrations

Table 3. Features of the bottom sediment core, VER-16-01, GC.4

Feature	Core layer, cm							
	0	10-15	40	50	100	200	250	274
Moisture, %	70	60	61	63	60	46	40	40
Total carbon content, %	5.1	5.1	7.7	7.5	5.6	2.7	2.9	2.6
Oil content, %	0.47	0.64	2.5	2.9	0.20	0.18	0.36	0.34
Σ_{alk} in oil, ppm	1400	1700	780	1200	1500	920	3300	1400
$R_{alk} = \Sigma[C_8\text{-}C_{18}]/\Sigma[C_{19}\text{-}C_{29}]$	0.52	-	0.35	0.33	-	-	-	1.1
Σ_{PAH} in oil, ppm	400	460	510	550	890	870	1100	1400
Σ_{naph} in oil, ppm	44	58	12	9.0	74	56	180	250
Σ_{phen} in oil, ppm	230	270	450	370	590	580	530	760
BaP in oil, ppm	8.5	6.7	9.7	9.2	5.3	3.2	9.3	9.8
The An/(An + Ph) ratio	0.26	0.34	0.12	0.11	0.12	0.11	0.12	0.10
The Flu/(Flu + Pyr) ratio	-	-	0.23	0.21	0.32	0.31	0.32	0.30

3.3. Assessment of Baikal water pollution near the deep oil seep

The area of the water surface covered with oil slicks at the site of the oil seepage near Cape Gorevoy Utes in 2016 and 2019 did not change in comparison with the 2005 data (Khlystov et al., 2007) and was ~1 km^2. In the surface water layer (without oil slicks), the Σ_{alk} concentration almost has not changed over 15 years since the discovery of this phenomena and ranges from 0.3 to 8.3 μg/L, with an average value of 3.6 μg/L and median of 3.0 μg/L (Fig. 3). Except for some samples, for example, from the 200 m layer at station R4, the concentration of the detected *n*-alkanes does not exceed the maximum permissible concentration (MPC_{fish} = 50 μg/L) established for monitoring petroleum hydrocarbons in water bodies of fishery importance (The list of fishery standards…, 1999) and is 25 to 40 times lower than the concentration of aliphatic hydrocarbons in the waters of the Atlantic and Southern oceans (Nemirovskaya, 2004).

Oil can enter the water column from different channels, such as asphalt structures resulting from oil fractionation at the water-bottom interface (Gorshkov et al., 2020), cracks and faults at the bottom of the lake, emitting separate oil balls at the bottom of the lake (Khlystov et al., 2009). In the latter case, the oil may enter the water column with minimal fractionation. The detection of extreme concentrations of *n*-alkanes and PAHs in the sample from the 200 m layer (station R4) may be the result of a similar oil discharge to lake waters and inclusion into the sample of water hydrocarbon plume that ascended through the water column to the surface of the lake.

The fraction of PAHs in the water column did not contain high molecular weight polyarenes with carcinogenic properties (BaP and DahA). In particular, BaP was not identified above the 0.02 MPC, which is established for this pollutant in drinking water: MPC_{EU} BaP = 10 ng/L (Council Directive 98/83/EC, 1988); MPC_{RUSSIA} BaP = 5 ng/L (SanPIN 2.1.4.1074-01.2001, 2002).

For PAHs found in the water column, total toxic equivalent (ΣTEQ) values ranged from 0.004 to 0.110 ng/L (Fig. 4). The maximum ΣTEQ values were observed for the PAH fraction in the bottom water layer (860 m), in which naphthalenes dominated. Contribution of naphthalenes to ΣTEQ is rated at 50-60%. The presence of An, Chr and BbF in water, which have relatively high toxicity coefficients (TEFs), also significantly contribute to the total TEQ of PAHs in this water layer. On a water surface covered with oil slicks, the toxicity of PAHs reaches a total TEQ of 100-200 ng/L. In the water of the upper water layer (5 m), ΣTEQ does not exceed 0.110 ng/L. Deep water (R4, 400 m) is characterised by a minimum level of total TEQ (0.004 ng/L), which is comparable to the toxicity assessment of PAHs in water samples collected at the reference station in the Baikal pelagic zone. In the absence of oil slicks on the water surface (station R6, 0 m), the ΣTEQ of PAHs is 0.055 ng/L. (St.3; Fig. 1).

The distribution of petroleum hydrocarbons in Baikal water from the site of deep seepage is limited, and water pollution is localised. The total concentrations of *n*-alkanes at the reference station (St.1, $\Sigma_{alk} \leq 0.15$ μg/L; Russell and Rosell-Mele, 2005; Gorshkov et al., 2010) are up to 35 times lower than the maximum Σalk concentrations found in the water column and on the water surface near Cape Gorevoy Utes. PAH concentrations in the surface water layer at sites without oil slicks on the surface and deep layers are comparable with Σ_{PAH} concentrations at reference stations and in the pelagic zone (7.0–36 ng/L; Gorshkov et al., 2018).

The low level of water pollution due to petroleum hydrocarbons near deep oil seepage sites is associated with natural mechanisms in the Baikal ecosystem. Microorganisms and phytoplankton make a decisive contribution to the purity of Baikal water, and oil fractionation during deep discharge contributes to the bioavailability of petroleum hydrocarbons. Model experiments indicated that during the cultivation of Baikal microorganisms in the presence of oil as a carbon source, *n*-alkanes and PAHs effectively degrade. Moreover, diatoms *Synedra acus* subsp. *radians*, the dominant species of Baikal phytoplankton, accumulate PAHs in their lipid bodies (Pavlova et al., 2005; 2012; Shishlyannikov et al., 2017; Gorshkov et al., 2020).

In the model experiments on oil degradation, there was no selective destruction of *n*-alkanes, and conversion of the fraction of normal hydrocarbons showed a simultaneous decrease in the content of all homologues. Therefore, the dominance of light *n*-alkanes in the water at sites with oil seepage is likely to be the result of oil fractionation at the bottom-water interface.

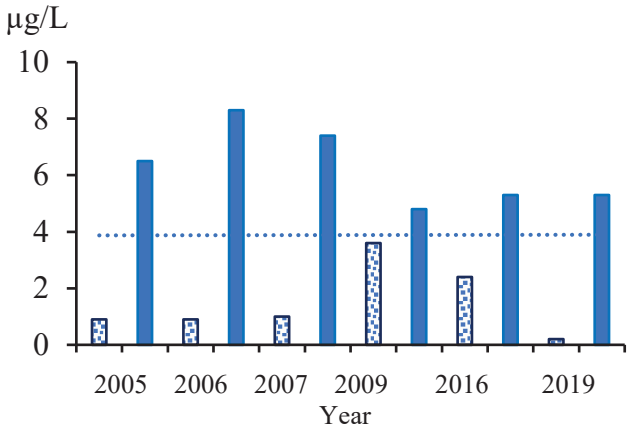

Fig.3. The trend of the content of n-alkanes in the surface water layer (without oil slicks) near the oil seep in 2005 – 2019, minimum and maximum Σ_{alk} concentrations, MPCfish = 50 μg/L

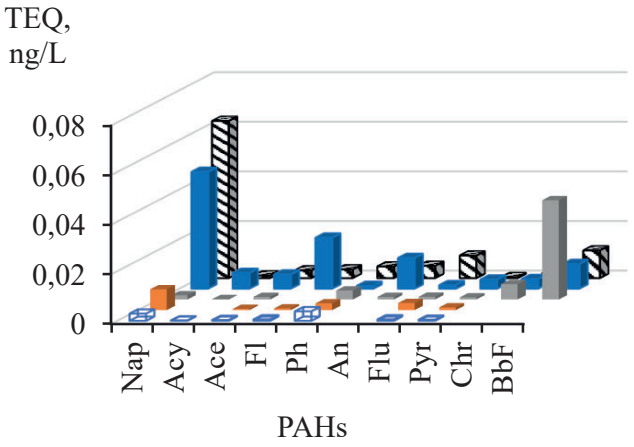

Fig. 4. Toxicity assessment of PAHs in the water column at the site of the oil seepage near Cape Gorevoy Utes:
- station R4, 400 m: Σ_{PAH} 14 ng/L, ΣTEQ 0.004;
- station R6, 0 m: Σ_{PAH} 14 ng/L, ΣTEQ 0.055;
- station R10, 5 m: Σ_{PAH} 90 ng/L, ΣTEQ 0.113;
- station R7, 860 m: Σ_{PAH} 100 ng/L, ΣTEQ 0.100
- station St.3, 5-1500 m (reference station in the Lake Baikal pelagic zone): Σ_{PAH} 10-27 ng/L, ΣTEQ 0.013-0.018

Perhaps, the ability to degrade hydrocarbons is fixed in the genomes of Baikal microorganisms inhabiting areas of natural oil seepage (Likhoshvay et al., 2013; Lomakina et al., 2014), because, owing to geological processes, oil and its deformation products are permanent components in the ecosystem of the east coast of the Central Baikal basin. Additionally, Baikal microorganisms synthesise surfactants (Pavlova et al., 2010); hence, biosurfactants can contribute to the sorption of hydrocarbons on suspended particles in Baikal water and subsequent deposition on the lake bottom.

The presence of *n*-alkanes and PAHs in Baikal water is due to not only natural sources but also technogenic sources, i.e. surface runoff, emissions

from vessels of the Baikal fleet, and emissions into the atmosphere from industrial enterprises along the coast. In the latter case, the Σ_{PAH} concentration in the surface water layer near the Listvyanka settlement can reach 160 ng/L, and in the Selenga River delta, the total concentration of petroleum hydrocarbons was 16–78 μg/L (St.1, St.2; Gorshkov et al., 2010).

4. Conclusion

The oil concentrates mainly on the water surface in the form of oil slicks. The area of the lake covered with oil slicks is ~1 km^2, and it almost has not changed since the discovery of oil seep in 2005. From 2005 to 2019, the concentration of *n*-alkanes in the surface water ranged between 0.2 and 8.3 μg/L, with an average value of 3.6 μg/L. The concentration of *n*-alkanes does not exceed 0.1 MPC_{fish} (MPC_{fish} = 50 μg/L), which was established for monitoring petroleum hydrocarbons in water bodies of fishery importance. The Σ_{PAH} concentration was within the range from 1.0 to 110 ng/L, and the fraction of PAHs detected there had no carcinogens. In particular, BaP was not identified above the 0.01–0.02 MPC, which had been established for this pollutant in drinking water (MPC_{EU} BaP = 10 ng/L, MPC_{RUSSIA} BaP = 5 ng/L). The toxicity of PAHs in oil slicks on the water surface had the TEQ value from 100 to 200 ng/L. For the PAHs found in the water column, TEQ values ranged from 0.004 to 0.110 ng/L. Deep water (400 m) is characterised by a minimum level of total TEQ, which is comparable to the assessment of the toxicity of PAHs in water samples collected at the reference station in the Baikal pelagic zone. The distribution of petroleum hydrocarbons in Baikal water from the site of deep seepage is limited, and water pollution is localised. At reference stations in the Baikal pelagic zone, the total concentrations of *n*-alkanes in the surface water layer are up to 35 times lower than that at the seepage site. The concentrations of PAHs in the surface water layer and deep layers in the pelagic zone of Lake Baikal range from 7.0 to 36 ng/L.

Acknowledgments

This work was conducted within the framework of the State Task, projects No. 0345–2019–0007 (*AAAA-A16-116122110064-7*) and No. 0345–2019–0008 (*AAAA-A16-116122110065-4*). The chromato-mass-spectrometric analysis was conducted at the Collective Instrumental Centre “Ultramicroanalysis”.

References

Council Directive 98/83/EC of 3 November, 1988. 1988. On the quality of water in intended for human consumption» into the national laws in the EU association countries. Official Journal of the European Communities 5.

Golmshtok A.Y., Duchkov A.D., Hutchinson D.R. et al. 2000. Heat flow and gas hydrates of the Baikal Rift Zone. International Journal of Earth Sciences 89: 193-211. DOI: 10.1007/s005319900071

Gorshkov A.G., Grachev M.A., Zemskaya T.I. et al. 2006. Oil in Lake Baikal, paradox or regularity? In: International Congress on Analytical Sciences, pp. 375-376.

Gorshkov A.G., Marinayte I.I., Zemskaya T.I. et al. 2010. Modern level of petroleum products in water of Lake Baikal and its tributaries. Chemistry for Sustainable Development 18: 623-630.

Gorshkov A.G., Kustova O.V., Izosimova O.N. et al. 2018 POPs monitoring system in Lake Baikal – impact of time or the first need? Limnolgy and Freshwater Biology 1: 43-48. DOI: 10.31951/2658-3518-2018-A-1-43

Gorshkov A.G., Pavlova O.N., Khlystov O.M. et al. 2020. Fractioning of petroleum hydrocarbons from seeped oil as a factor of purity preservation of water in Lake Baikal. Journal of Great Lakes Research 46: 115-122. DOI: 10.1016/j.jglr.2019.10.010

Hazen T.C., Dubinsky E.A., DeSantis T.Z. et al. 2010. Deep-sea oil plume enriches indigenous oil-degrading bacteria. Science 330: 204-208. DOI: 10.1126/science.119597

Kashirtsev V.A., Kontorovich A.E., Moskvin V.I. et al. 2006. Terpanes from oil shows of Lake Baikal. Petroleum Chemistry 46: 217-224. DOI: 10.1134/S0965544106040013

Khlystov O.M., Gorshkov A.G., Egorov A.V. et al. 2007. Oil in the lake of world heritage. Doklady Earth Sciences 414: 635-659. DOI: 10.1134/S1028334X07050042

Khlystov O.M., Zemskaya T.I., Sitnikova T.Y. et al. 2009. Bottom bituminous constructions and biota inhabiting them according to investigation of Lake Baikal with the mir submersible. Doklady Earth Sciences 429: 1333-1336. DOI: 10.1134/S1028334X09080200

Kontorovich A.E., Kashirtsev V.A., Moskvin V.I. et al. 2007. Petroleum potential of Baikal deposits. Russian Geology and Geophysics 48: 1046-1053. DOI: 10.1016/j.rgg.200 7. 11.004

Likhoshvay A., Khanaeva T., Gorshkov A. et al. 2013. Do oil–degrading *Rhodococci* contribute to the genesis of deep-water bitumen mounds in Lake Baikal? Geomicrobiology Journal 30: 209-213. DOI: 10.1080/01490451.2012.665149

Lomakina A.V., Pogodaeva T.V., Morozov I.V. et al. 2014. Microbial communities of the discharge zone of oil- and gas-bearing fluids in low-mineral Lake Baikal. Microbiology 83: 278-287. DOI: 10.1134/S0026261714030126

Nemirovskaya I.A. 2004. Uglevodorody v okeane (sneg - led - voda - vzves’ - donnyye osadki) [Hydrocarbons in the ocean (snow-ice-suspended matter-bottom sediments)]. Moscow: Nauchnyj Mir. (in Russian)

Nisbet I.C.T., LaGoy P.K. 1992. Toxic equivalency factors (TEFs) for polycyclic aromatic hydrocarbons (PAHs). Regulatory Toxicology and Pharmacology 16: 290-300. DOI: 10.1016/0273-2300(92)90009-x

Pavlova O.N., Parfenova V.V., Zemskaya T.I. et al. 2005. Biodegradation of oil and hydrocarbon by microbial community of Lake Baikal. In: The IV-th Vereshchagin Baikal Conference, p. 147. (in Russian)

Pavlova O.N., Lomakina A.V., Likhoshvay A.V. et al. 2010. Microbial communities in areas of natural oil outflow on Lake Baikal. Uspekhi Nauk o Zhizni [Successes in Life Sciences] 2: 169-172. (in Russian)

Pavlova O.N., Lomakina A.V., Gorshkov A.G. et al. 2012. Microbial communities and their ability to oxidize n-alkanes in the area of release of gas and oil containing fluids in mid-Baikal (cape Gorevoi Utes). Biology Bulletin 39: 458-463. DOI: 10.1134/S1062359012050123

Russell M., Rosell-Mele A. 2005. Preliminary study of fluxes of major lipid biomarker classes in the water column and sediments of Lake Baikal, Russia. Global and Planetary Change 46: 45-56. DOI: 10.1016/j.gloplacha.2004.11.005

SanPIN 2.1.4.1074-01.2001. 2002. Drinking water. Hygienic requirements water quality of centralised drinking

water supply systems. Quality control. Resolution No 24. September 26. (in Russian)

Shishlyannikov S.M., Nikonova A.A., Klimenkov I.V. et al. 2017. Accumulation of petroleum hydrocarbons in intracellular lipid bodies of the freshwater diatom *Synedra acus* subsp. *Radians*. Environmental Science Pollution Research 24: 275-283. DOI: 10.1007/s11356-016-7782-y

Simoneit B.R.T., AboulKassim T.A.T., Tiercelin J.J., 2000. Hydrothermal petroleum from lacustrine sedimentary organic matter in the East African Rift. Applied Geochemistry 15: 355-368. DOI: 10.1016/S0883-2927(99)00044-X

The list of fishery standards for maximum permissible concentrations (MPC) and tentatively safe exposure levels (SEC) of harmful substances for water of water bodies of fishery importance. 1999. Moskow: VNIRO. (in Russian)

Vila J., Nieto J.M., Mertens J. et al. 2010. Microbial community structure of a heavy fuel oil-degrading marine consortium: linking microbial dynamics with polycyclic aromatic hydrocarbon utilization. FEMS Microbial Ecology 73: 349-362. DOI: 10.1111/j.1574-6941.2010.00902.x

Zarate-del Valle P.F., Rushdi A.I., Simoneit B.R.T. 2006. Hydrothermal petroleum of Lake Chapala, Citala Rift, western Mexico: bitumen compositions from source sediments and application of hydrous pyrolysis. Applied Geochemistry 21: 701-712. DOI: 10.1016/j.apgeochem.2006.01.002

Yender R., Stanzel K. 2011. Tanker SOLAR 1 Oil spill, Guimaras, Philippines: impacts and response challenges. In: Fingas M.F. (Ed.), Oil spill science and technology. Prevention, response, and cleanup. Burlington, pp. 1133-1146.

Yunker M.B., Macdonald R.W., Vingarzan R. et al. 2002. PAHs in the Fraser River basin: a critical appraisal of PAH ratios as indicators of PAH source and composition. Organic Geochemistry 33: 489-515. DOI: 10.1016/ S0146-6380(02)00002-5

Limnology and Freshwater Biology 2020 (2): 405-411 DOI:10.31951/2658-3518-2020-A-2-405

Original Article

ISSN 2658-3518
LIMNOLOGY FRESHWATER BIOLOGY
www.limnolfwbiol.com

The phylogeny based on the intron of ATP synthase α-subunit gene reveals a substrate role in the origin of the gastropod species flock from Lake Baikal

Kovalenkova M.V.[1]*, Bukin Yu.S.[1, 2], Sitnikova T.Ya.[1], Sherbakov D.Yu.[1, 2]

[1] *Limnological Institute, Siberian Branch of the Russian Academy of Sciences, Ulan-Batorskaya Str., 3, Irkutsk, 664033, Russia*
[2] *Irkutsk State University, Karl Marx Str., 1, Irkutsk, 664003, Russia*

ABSTRACT. A nuclear marker, an intron of ATP synthase α-subunit gene, used to determine phylogenetic relationships between 22 species of the family Baicaliidae (Caenogastropoda: Rissooidea) indicated two genetic groups of these gastropods in Lake Baikal. The obtained groups partially coincide with the clusters revealed by the mitochondrial COI gene and do not fully coincide with the modern taxonomy of the family. Thirteen species of the first group inhabit different sediments (silty sand, sand, stones, and rocks), eight out of the nine species from the second group are psammobionts. Both genetic groups include eurybathic and stenobathic species widely distributed in the North, Middle and Southern Basins of the lake, as well as species, whose habitats are limited to one or two basins. Phylogenetic analysis suggests that the main way of baicaliids speciation was the repeated occupation of the same habitats by different ancestral forms. Sculpture of the shells (ribs, carina and/or periostracal hairs/plates) also most likely appeared independently in each group due to similar adaptation.

Keywords: substrate preferences, sand-dwelling, Baicaliidae

1. Introduction

The processes generating the unique biodiversity in ancient lakes remain not quite clear, giving rise to numerous hypotheses (Cristescu et al., 2010). In the understanding of the driving forces of evolution, of particular interest are the processes leading to the rapid emergence of a large number of closely related species (species flocks) (Brooks, 1950). In ancient lakes, periods of intense speciation is normally associated with the consequences of some rapid catastrophic changes that caused the formation of a large number of new and/or unpopulated ecological niches (Martens, 1997; Sherbakov, 1999; Kroll et al., 2012; Miura et al., 2019). During adaptive radiation morphological, environmental and behavioral characteristics of closely related organisms can change very quickly (Martin and Wainwright, 2011).

The endemic gastropods of the family Baicaliidae (Fischer 1885) include more than 40 species belonging to 8 genera and it is the largest species flock among gastropods from ancient lakes. Family or subfamily rank of this group has been considered (Wilke, 2004; Wilke et al., 2013; Vinarski and Kantor, 2016). Baicaliids are found on all types of sediments at the depth from 1.5 to 250 m, most species were collected at the depths down to 50 m (Kozhov, 1936; Sitnikova et al., 2004). Some species widely distributed in the lake; the habitat of a few species is limited to one-two basins or a single geographical part (northern or southern) of the lake. There are pairs of species (or subspecies) of similar shell morphology and occupying similar habitats but in different lake basins (Kozhov, 1936; Sitnikova, 2006). Sympatric distributed species differ in time of reproduction (Sitnikova et al., 2001), reproductive behavior (Sitnikova, 2004) or trophic preferences (Sitnikova et al., 2012). Previously diversification within macro- and microhabitats was proposed as the main way of the speciation of the Baikal endemic gastropods (Starobogatov and Sitnikova, 1990).

The relative evolutionary youth of contemporary baicaliids and rapid evolution significantly complicate the study of their phylogenetic relationships (Zubakov et al., 1997). Analysis of polymorphism of cytochrome c oxidase gene (COI) fragment in 25 species indicated two genetic baicaliid clusters that do not fully correspond to the taxonomy of the family based on morphological characteristics (Zubakov, 1999). The morphological variability of the shells in the members of the family suggests the presence of transitional forms and interspecific hybrids (Kozhov, 1936). Furthermore, the intraspecific genetic variation of the COI gene in some species exceeds interspecific differences (Peretolchina et al., 2007). The intron of the nuclear ATP synthase

*Corresponding author.
E-mail address: mkovalenkova@gmail.com (M.V. Kovalenkova)

α-subunit gene served in our study as a variable and neutral marker for the evolution of baicaliids (Kovalenkova et al., 2015) because the mitochondrial genome may undergo frequent events of different types of genetic selection being a single segregation unit due to lack of recombination (Chong et al., 2016; Sun et al., 2017).

This study aims to evaluate the intron variability of the ATP synthase α-subunit gene in gastropods of the family Baicaliidae as well as the relationship of genetic polymorphism with some known environmental and morphological characteristics of species.

2. Materials and methods

Gastropods belonging to all baicaliid genera were collected in 2006–2017 with dredging and scuba diving from 22 littoral and sublittoral sites (5-40 m) (Table).

Shells were photographed before dissecting. We isolated genomic DNA from foot tissues using a CTAB procedure described by Doyle and Dikson excluding isoamyl alcohol adding (1987).

Intron-containing partial fragment of ATP synthase α-subunit gene was obtained using primers universal for coelomate animals (Jarman et al., 2002). Thermocycling conditions were as follows: 94 °C – 2 min, 35 cycles: 94 °C – 20 s, 54 °C – 1 min, 72 °C – 1 min (with a final elongation step of 3 min). PCR products of the intron were separated on 1% agarose gel and purified using the freeze-squeeze method (Tautz and Renz, 1983). Then the amplification products were sequenced at JSC Sintol (Moscow). GenBank accession numbers are shown in Table.

Sequenograms were edited and aligned with Geneious v. 9.0.5 (Kearse et al., 2012). Double peaks were named according to IUPAC nomenclature with Heterozygotes plugin (Geneious) using a threshold of 50% peak height. Intron alleles for heterozygous specimens were twice identified using the PHASE algorithm in DnaSP v. 5.10.01 (Librado and Rozas, 2009). Reconstruction results were the same. The best-fit model of sequence evolution was inferred based on the Bayesian information criterion with IQ-tree v. 1.6.10 (Nguyen et al., 2015).

Maximum Likelihood (ML) tree from unique alleles of the intron was constructed with IQ-tree v. 1.6.10. In order to assess the robustness of the tree topology, bootstrap node support values were estimated from 100 pseudoreplicates. ML tree have been inferred without an outgroup because of the lack of the sequence information for the ATP synthase α-subunit gene intron for any sister taxa.

Medians of paired interspecific genetic distances were estimated with the F81 + I model (Felsenstein, 1981) in the “ape” package R (Paradis et al., 2004). The statistical parsimony network (Templeton et al., 1992) was inferred with the fixed connection limit set to 97% in the “pegas” package R (Paradis, 2010).

Ecological characters (minimum and maximum habitat depths limits, substrate preferences, habitat area) and teleoconch sculpture characters were assigned according to Kozhov (1936) and Sitnikova (2004) (Table).

The relationship of environmental and morphological characteristics with genetic differentiation was assessed with non-metric multidimensional scaling (NMDS) using the matrix of median pairwise interspecific distances as source data. Qualitative and quantitative environmental and morphological characteristics served as grouping factors of species distribution in the space of NMDS coordinates to calculate the ratios of intra-factor and inter-factor variations for interspecific median distances, R2 ($R2 = 1 - ssw/sst$, where ssw and sst are within-group and total sums of squares). The greater the R2 value for the studied factor, the greater its influence on the degree of genetic differentiation between species. The reliability of the R2 value was calculated using 3000 repetitions of permutation test (Phipson and Smyth, 2010) and adjusted by the Benjamini and Hochberg method for multiple comparisons (Benjamini and Hochberg, 1995). If $P < 0.05$ then R2 significantly differs from zero, and the influence of the factor on the interspecific genetic differentiation is considered reliable. The calculations were carried out using the “vegan” package R according to the recommendations of Oksanen (2015).

3. Results

We obtained the nucleotide sequences of the intron of the ATP synthase α subunit gene for 55 specimens belonging to 22 species (1-6 specimens per species). The intron length varied from 466 to 523 bp in different species due to short insertions and deletions (indels). Half of the indels (11 of 22) occur in short mononucleotide tracts and paired tandem repeats, which may serve as hotspots for replication slippage (Clayton et al., 2016). Such mutations may occur independently in different lineages, distorting the phylogenetic signal, and in the analysis of genetic distances, we used only the information about nucleotide substitutions.

Three specimens had allele pair probabilities < 0.95 (Table 1), unique alleles from these specimens shown on the network with single alleles of *Parabaikalia dubiosa* and *Korotnewia semenkewitschii* (Fig.). Genotypes are sufficient for interspecific genetic distances estimates therefore rare alleles were not excluded from the analysis.

Genetic distances between 43 unique intron alleles in pairwise comparisons are from 0.19% to 3.86%. Intraspecific distances vary from 0 to 0.8% of nucleotide substitutions. Moreover, we found two shared alleles. The first one occurs in representatives of closely related *Korotnewia angygira* and *K. korotnewi* from different localities. The second shared allele has a central position in the phylogenetic network and was found in the members of the species *Teratobaikalia ciliata* and *Pseudobaikalia zachwatkini* which significant differ morphologically. The presence of the common alleles is likely owing to the retention of ancestral polymorphism.

Table. Ecological and teleoconch sculpture characters of Baicaliidae species and specimens examined in this study.

Species	Minimum depth	Maximum depth	Basin	Substrate	Hair	Ribs	Collection sites	GenBank no.
Baicalia carinata	15	100	a	m	n	n	Arul, Yakshakan, Semisosennaya	KF201695-KF201697
Baicalia dybowskiana	3	80	a	m	n	y	Semisosennaya	KF201698
Baicalia turriformis	10	40	s	r	n	y	Polovinnaya	KT885112
Godlewskia wrzesniowski	15	120	s	s	n	y	Olkhon gate	KF201707
Korotnewia angigyra	11	100	n	s	y	n	Barguzinsky gulf	KF201706
Korotnewia korotnewii	10	120	a	s	y	n	Olkhon gate, Senogda bay	KT885113, MT261207- MT261210
Korotnewia semenkewitschi	2	100	a	s	y	n	Barguzinsky gulf, Ayaya, Goloustnoe	KF201705, MT261211- MT261212*
Liobaikalia stiedae	15	120	s	s	y	n	Listvyanka, Utulik	KT885093, MT261218
Maackia herderiana	1	20	s	r	n	y	Listvyanka	KF201699
Maackia variesculpta	1	20	n	r	n	y	Arul	MT261226
Parabaikalia elata	4	20	a	s	n	n	Peschannaya bay	KF201704
Parabaikalia dubiosa	4	20	n	s	n	n	Boro-Elga, Olkhon gate, Nemnyanka	KT885102- KT885103*, MT261225*
Parabaikalia kobeltiana	5	30	s	s	y	n	Boro-Elga	KF201701
Parabaikalia oviformis	3	20	a	s	n	n	Peschannaya bay	KF201702, KF201703
Pseudobaicalia contabulata	10	40	a	s	n	y	Olkhon gate, Ayaya, Onokachanskaya	KT885109, MT261216- MT261217
Pseudobaicalia elegantula	1	15	n	m	n	y	Turkinskaya bank	MT261223
Pseudobaikalia jentteriana	15	100	n	s	n	n	Olkhon gate	KT885104, KT885105
Pseudobaikalia michelae	11	40	na	m	n	n	Kultuk, Barguzinsky gulf	KT885096-KT885101
Pseudobaikalia pulla	15	120	a	s	n	y	Olkhon gate, Listvyanka, Onokachanskaya, Svyatoy nos	KF201700, MT261224, KT885106-KT885108
Pseudobaicalia zachwatkini	3	30	a	m	n	y	Listvyanka, Onokachanskaya, Nizhneangarsk	KT885095, MT261213- MT261215
Teratobaikalia duthiersii	15	50	s	m	n	y	Kultuk	KF201709
Teratobaikalia ciliata	2	15	s	r	n	y	Polovinnaya, Listvyanka, Kedrovyy cape, Izhimey cape	KT885094, MT261219-MT261222

Basin: s – south; n –north; a – all area. Substrate: s – soft (mud and sand); r – hard; m – mixed. Hairs and ribs: y – present; n – not present. GenBank numbers of genotypes with allele pair probabilities <0.95 marked with an asterisk.

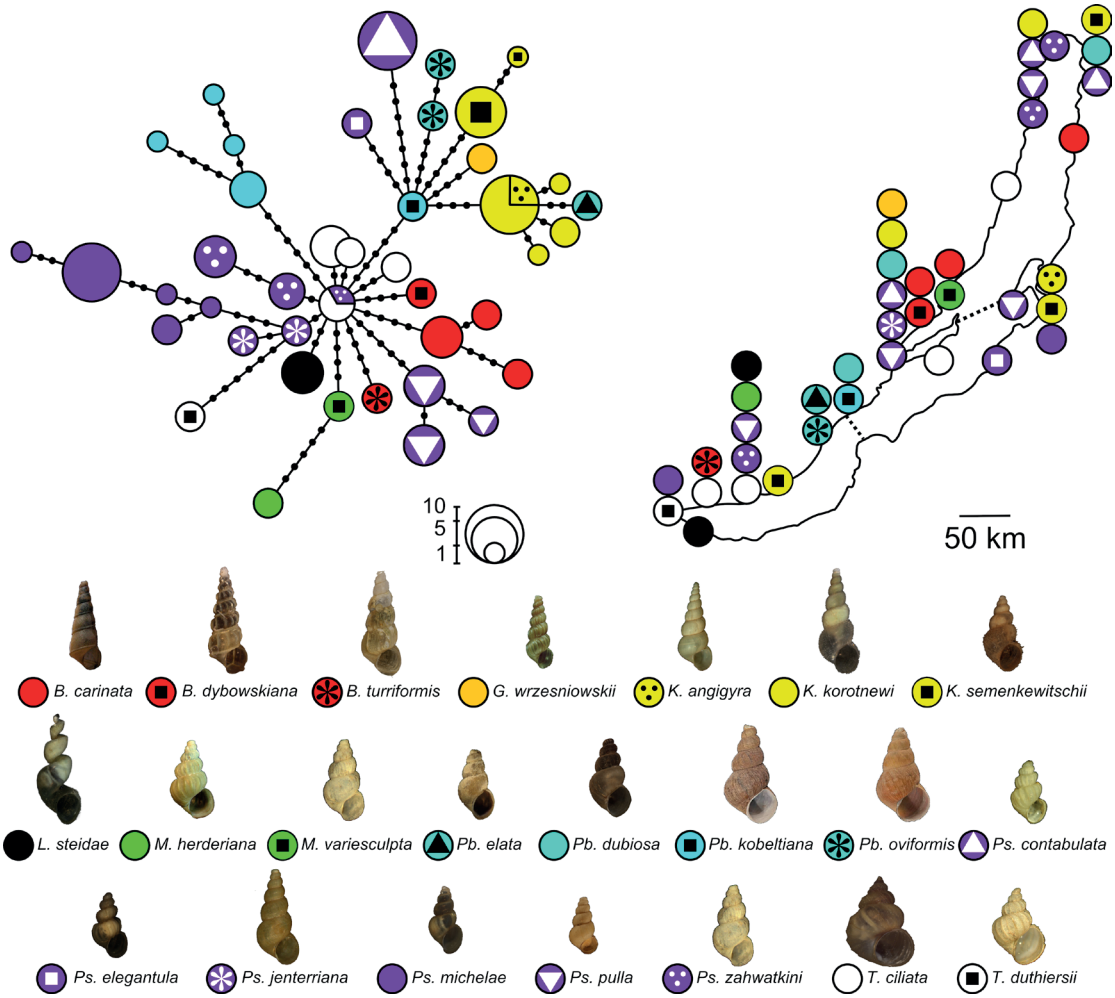

Fig.1. Intron allele network and localities for Baicaliidae species. Circle sizes are proportional to allele frequencies and colors represent the respective genera, species indicated by symbols. Dotted lines marked the boundaries of the Baikal basins.

Interspecific differences of intron sequences are small; at the same time, intraspecific polymorphism may be significant (Fig.). The star-like network topology allows to distinguish two genetic groups of baicaliids differing by at least four nucleotide substitutions.

Median interspecific distances are 1.36 ± 0.6% for the first group and 1.03 ± 0.65% – for the second group. The larger and more diverse genetically group includes 13 species: all members of the genera *Baicalia*, *Liobaikalia*, *Maackia*, *Teratobaikalia*, and *Pseudobaikalia*, except for *P. contabulata* and *P. elegantula*. In addition to the indicated exceptions, the second group includes the species of the genera *Godlewskia*, *Korotnewia* and *Parabaikalia*, except for *P. dubiosa*. Therefore, the members of two genera, *Parabaikalia* and *Pseudobaikalia*, appear in both genetic groups. Notably, only one and two species represent the genera *Godlewskia*, *Maackia* and *Teratobaikalia*, which is less than a third of their species diversity.

The species from the first group differ in their substrate preferences. Four of them are strict psammobionts: *L. stiedae*, *P. dubiosa*, *P. jentteriana*, and *P. pulla*; the other four belong to strict lithobionts: *B. turriformis, M. herderiana, M. variesculpta*, and *T. ciliata*. The remaining five species are found on various types of substrates (*B. carinata*, *P. elegantula* and *P. michelae*) or migrate during the breeding season from sand to stones (*B. dybowskiana* and *T. duthiersii*).

In the second group, only one of the nine species inhabits mixed-type substrates. *P. elegantula* inhabits the bottom side of large stones and boulders lying on the sand. Thus, this is a group with predominantly psammobiontic species. ML tree contains the same well-supported clades (BS = 77 for both).

The only factor that differentiates the interspecific distances is the preferred substrate of the baicaliids species ($R2 = 0.35$, $p = 0.018 < 0.05$ after correction). Minimum and maximum depths, shell sculpture or geographical distribution do not significantly discriminate phylogenetic species relatedness.

4. Discussion and conclusions

Intron allele network topology indicates two genetic groups of baicaliids. One group consists of the species adapted to highly diverse habitats on different sediments, while most members of the second group occupy various habitats on sandy substrates. Psammobiont species of both groups include species as able to burrow in soft substrates as species actively move along the surface of soft sediments. Ribs and periostracal hairs (or plates of various shapes) on the shell also occur in representatives of both groups. Additionally, the degree of manifestation of these morphological

characteristics can vary at the intraspecific level (Kozhov, 1936; Sitnikova and Maximova, 2015). Therefore, adaptations to the same environments in the two groups could evolve independently. Data on the food composition of sandy living baicaliids is scarce (Roepstorf et al., 2003), meanwhile, by analogy with "rocky" species (Sitnikova et al., 2012), we suggest that co-existent "sandy" species consume different foods.

The species diversity of the psammobiont clade suggests the significance of the variety of microhabitats and the corresponding trophic adaptations that exist on soft substrates. One of the likely reasons for the formation of the observed diversity may be also preadaptation in the ancestor of psammobiont group, due to which it was more difficult for its members to adapt to habitat on the stony substrates.

One of the most interesting examples illustrating the influence of substrates on the diversification of species flock is cichlids from Lake Malawi where one of the genetic lineages inhabits sandy substrates, and another – the stony ones. A study of this species flock is explained by a three-stage hypothesis of the species flock development, according to which the speciation at the initial stage occurs when different substrates are occupied (Streelman and Danley, 2003). This is followed by separation according to trophic preferences, and at the final stage of the species flock diversification sexual selection takes place (Santos-Santos et al., 2015; Malinsky and Salzburger, 2016). The applicability of this model remains controversial (Hulsey et al., 2017), although it has become widespread for many groups of organisms (Ackerly et al., 2006; Leaché et al., 2016; Veríssimo et al., 2017). Perhaps, this example represents an individual case of phylogenetic niche conservatism (PNC) when closely related species occupy similar niches (Hopkins et al., 2014; Morinière et al., 2016).

The reasonable explanation for the evolution of the observed baicaliid diversity may be the change in the availability of different substrates during the development of the Baikal Rift. Estimates of the baicaliids divergence times about 2.5-4.3 (Zubakov, 1999; Mats et al., 2011) coincide with the beginning of the climatic and geomorphological changes (Kachukov et al., 1998; Mats and Yefimova, 2011). The terrestrial and underwater relief experienced great transformations ca. 4-3 which led to the sedimentation pattern changes as well as to a decrease in the availability of soft substrates, especially along the west coast (Mats and Yefimova, 2011). Over time, soft substrates restored, which could promote the diversification of a psammobiont clade.

In some other ancient lakes, the rapid speciation of endemic caenogastropods also coincided with great geological changes. For instance, significant changes in the level and salinity of Lake Titicaca and the preceding paleolakes coincide in time with the diversification of the species flock within the genus *Heleobia* (Kroll et al., 2012). In Lake Biwa, endemic gastropods of the genus *Semisulcospira* (*Biwamelania*) formed two species flocks whose ancestors appeared in the lake at different times. Nevertheless, the difference in niches (different types of substrates and depths) was simultaneous in both lineages in response to the lake expansion (Miura et al., 2019).

The composition of the two identified genetic groups of baicaliids does not fully correspond to the existing taxonomy and phylogenetic reconstructions based on a mitochondrial marker (Zubakov, 1999; Sitnikova, 2004). Though both molecular phylogenies show the relatedness of members of the genera *Korotnewia* and *Parabaikalia* as well as polyphyly of the genus *Pseudobaikalia*. Previous phylogenetic analysis of the intron of ATP- synthase alpha-subunit gene from 11 baicaliid species shows similar results (Kovalenkova et al., 2015). However, extended data set presented here shows that even very morphologically different species can have small genetic distances maybe due to the retention of ancestral polymorphism (for example in the case of *P. zahwatkini* and *T. ciliata*).

However, our phylogenetic conclusions are also based on one genetic locus, and the existing evolutionary relationships between sister species may not be correctly interpreted. There are several examples of mismatch in the degree of genetic relatedness of baicaliids evaluated using markers with different cellular localization (Peretolchina et al., 2007; Sitnikova et al., 2016; Sherbakov et al., 2017). Obtaining the most complete information about the processes of baicaliid speciation requires the use of several variable and unlinked genetic markers.

Acknowledgments

This work was supported by the state project of LIN SB RAS No. 0345-2019-0004 (AAAA-A16-116122110060-9). We thank A.B. Kupchinsky, I.V. Khanaev, I.A. Nebesnykh, Yu. Yushuk and V.I. Chernykh for their assistance in sampling.

References

Ackerly D.D., Schwilk D.W., Webb C.O. 2006. Niche evolution and adaptive radiation: testing the order of trait divergence. Ecology 87: 50-61. DOI:10.1890/0012-9658(2006)87[50:NEAART]2.0.CO;2

Benjamini Y., Hochberg Y. 1995. Controlling the false discovery rate: a practical and powerful approach to multiple testing. Journal of the Royal Statistical Society: Series B (Methodological) 57: 289-300. DOI: 10.1111/j.2517-6161.1995.tb02031.x

Brooks J.L. 1950. Speciation in ancient lakes. The Quarterly Review of Biology 25: 131-176. DOI: 10.1086/397539

Chong J.P., Harris J.L., Roe K.J. 2016. Incongruence between mt DNA and nuclear data in the freshwater mussel genus *Cyprogenia* (Bivalvia: Unionidae) and its impact on species delineation. Ecology and Evolution 6: 2439-2452. DOI: 10.1002/ece3.2071

Clayton A.L., Jackson D.G., Weiss R.B. et al. 2016. Adaptation by deletogenic replication slippage in a nascent symbiont. Molecular Biology and Evolution 33: 1957-1966. DOI: 10.1093/molbev/msw071

Cristescu M.E., Adamowicz S.J., Vaillant J.J. et al. 2010. Ancient lakes revisited: from the ecology to the genetics of speciation. Molecular Ecology 19: 4837-4851. DOI: 10.1111/j.1365-294X.2010.04832.x

Doyle J.J., Dickson E. 1987. Preservation of plant samples for DNA restriction endonuclease analysis. Taxon 36:

715-722. DOI: 10.2307/1221122

Felsenstein J. 1981. Evolutionary trees from DNA sequences: a maximum likelihood approach. Journal of Molecular Evolution 17: 368-376. DOI: 10.1007/BF01734359

Hopkins M.J., Simpson C., Kiessling W. 2014. Differential niche dynamics among major marine invertebrate clades. Ecology Letters 17: 314-323. DOI: 10.1111/ele.12232

Hulsey C.D., Zheng J., Faircloth B.C. et al. 2017. Phylogenomic analysis of Lake Malawi cichlid fishes: further evidence that the three-stage model of diversification does not fit. Molecular Phylogenetics and Evolution 114: 40-48. DOI: 10.1016/j.ympev.2017.05.027

Jarman S.N., Ward R.D., Elliott N.G. 2002. Oligonucleotide primers for PCR amplification of coelomate introns. Marine Biotechnology 4: 347-355. DOI: 10.1007/s10126-002-0029-6

Kachukov V., Lykov D., Pevzner L. et al. 1998. A continuous record of climate changes of the last 5 million years stored in the bottom sediments of Lake Baikal. Geologiya I Geofizika [Geology and Geophysics] 39: 139-156. (in Russian)

Kearse M., Moir R., Wilson A. et al. 2012. Geneious Basic: an integrated and extendable desktop software platform for the organization and analysis of sequence data. Bioinformatics 28: 1647-1649. DOI: 10.1093/bioinformatics/bts199

Kozhov M.M. 1936. Mollyuski ozera Baikal: sistematika, raspredeleniye, ekologiya, nekotoryye dannyye po genezisu i istorii [Molluscs of Lake Baikal: systematics, distribution, ecology, some data on the genesis and history]. Moscow-Leningrad: USSR Academy of Sciences Publishing House. (in Russian)

Kovalenkova M.V., Sitnikova T.Y., Sherbakov D.Y. 2015. Genetic and morphological diversification in gastropods of the Baicaliidae family. Russian Journal of Genetics: Applied Research 5: 110-117. DOI: 10.1134/S2079059715020045

Kroll O., Hershler R., Albrecht C. et al. 2012. The endemic gastropod fauna of Lake Titicaca: correlation between molecular evolution and hydrographic history. Ecology and Evolution 2: 1517-1530. DOI: 10.1002/ece3.280

Leaché A.D., Banbury B.L., Linkem C.W. et al. 2016. Phylogenomics of a rapid radiation: is chromosomal evolution linked to increased diversification in north american spiny lizards (Genus *Sceloporus*)? BMC Evolutionary Biology 16: 63. DOI: 10.1186/s12862-016-0628-x

Librado P., Rozas J. 2009. DnaSP v5: a software for comprehensive analysis of DNA polymorphism data. Bioinformatics 25: 1451-1452. DOI: 10.1093/bioinformatics/btp187

Malinsky M., Salzburger W. 2016. Environmental context for understanding the iconic adaptive radiation of cichlid fishes in Lake Malawi. Proceedings of the National Academy of Sciences 113: 11654-11656. DOI: 10.1073/pnas.1614272113

Martens K. 1997. Speciation in ancient lakes. Trends in Ecology & Evolution 12: 177-182. DOI: 10.1016/S0169-5347(97)01039-2

Martin C.H., Wainwright P.C. 2011. Trophic novelty is linked to exceptional rates of morphological diversification in two adaptive radiations of *Cyprinodon* pupfish. Evolution: International Journal of Organic Evolution 65: 2197-2212. DOI: 10.1111/j.1558-5646.2011.01294.x

Mats V.D., Yefimova I.M. 2011. Paleogeographic scenario of the Late Cretaceous-Cenozoic for the central part of the Baikal region. Geodinamika i Tektonofizika [Geodynamics & Tectonophysics] 2: 175-193. DOI: 10.5800/GT-2011-2-2-0040 (in Russian)

Mats V.D., Shcherbakov D.Y., Efimova I.M. 2011. Late Cretaceous-Cenozoic history of the Lake Baikal depression and formation of its unique biodiversity. Stratigraphy and Geological Correlation 19. DOI: 10.1134/S0869593811040058

Miura O., Urabe M., Nishimura T. et al. 2019. Recent lake expansion triggered the adaptive radiation of freshwater snails in the ancient Lake Biwa. Evolution Letters 3: 43-54. DOI: 10.1002/evl3.92

Morinière J., Van Dam M.H., Hawlitschek O. et al. 2016. Phylogenetic niche conservatism explains an inverse latitudinal diversity gradient in freshwater arthropods. Scientific Reports 6. DOI: 10.1038/srep26340

Nguyen L.T., Schmidt H.A., Von Haeseler A. et al. 2015. IQ-TREE: a fast and effective stochastic algorithm for estimating maximum-likelihood phylogenies. Molecular Biology and Evolution 32: 268-274. DOI: 10.1093/molbev/msu300

Oksanen J. 2015. Vegan: an introduction to ordination. URL http://cran. r-project. org/web/packages/vegan/vignettes/introvegan. pdf, 8, 19.

Paradis E. 2010. Pegas: an R package for population genetics with an integrated–modular approach. Bioinformatics 26: 419-420. DOI: 10.1093/bioinformatics/btp696

Paradis E., Claude J., Strimmer K. 2004. APE: analyses of phylogenetics and evolution in R language. Bioinformatics 20: 289-290. DOI: 10.1093/bioinformatics/btg412

Peretolchina T.E., Bukin Y.S., Sitnikova T.Y. et al. 2007. Genetic differentiation of the endemic Baikalian mollusk *Baicalia carinata* (Mollusca: Caenogastropoda). Russian Journal of Genetics 43: 1400-1407. DOI: 10.1134/S1022795407120095

Phipson B., Smyth G.K. 2010. Permutation P-values should never be zero: calculating exact P-values when permutations are randomly drawn. Statistical Applications in Genetics and Molecular Biology 9. DOI: 10.2202/1544-6115.1585

Roepstorf P., Sitnikova T.Y., Timoshkin O.A. et al. 2003. Observation on stomach contents, food uptake and feeding strategies of endemic Baikalian gastropods. Berliner Paläobiologische Abhandlungen [Berlin Paleobiological Treatises] 4: 157-181.

Santos-Santos J.H., Audenaert L., Verheyen E. et al. 2015. Divergent ontogenies of trophicmorphology in two closely related haplochromine cichlids. Journal of Morphology 276: 860-871. DOI: 10.1002/jmor.20385

Sherbakov D.Y. 1999. Molecular phylogenetic studies on the origin of biodiversity in Lake Baikal. Trends in Ecology & Evolution 14: 92-95. DOI: 10.1016/S0169-5347(98)01543-2

Sherbakov D.Y., Kovalenkova M.V., Maikova O.O. 2017. Some results of molecular phylogenetic studies of Baikal endemic invertebrates. Russian Journal of Genetics: Applied Research 7: 345-349. DOI: 10.1134/S2079059717040104

Sitnikova T., Ropstorf P., Riedel F. 2001. Reproduction, duration of embryogenesis, egg capsules and protoconchs of gastropods of the family Baicaliidae (Caenogastropoda) endemic to Lake Baikal. Malacologia 43: 59-85.

Sitnikova T.Y. 2004. Prosobranch caenogastropoda molluscs (Gastropoda: Prosobranchia) from Baikal: morphology, taxonomy, biology and fauna origin. Dr. Sc. Dissertation, Irkutsk State University, Irkutsk, Russia. (in Russian)

Sitnikova T.Y. 2006. Endemic gastropod distribution in Baikal. Hydrobiologia 568: 207-211. DOI: 10.1007/s10750-006-0313-y

Sitnikova T., Maximova N. 2015. On morphological and ecological evidence of adaptive differentiation among stony cliff littoral Baikal gastropods. Journal of Natural History 50: 263-280. DOI: 10.1080/00222933.2015.1059961

Sitnikova T., Kiyashko S.I., Maximova N. et al. 2012. Resource partitioning in endemic species of Baikal gastropods indicated by gut contents, stable isotopes and radular morphology. Hydrobiologia 682: 75-90. DOI: 10.1007/s10750-011-0685-5

Sitnikova T., Kovalenkova M., Peretolchina T. et al. 2016. A new, genetically divergent species of *Pseudobaikalia*

Lindholm, 1909 (Caenogastropoda, Baicaliidae). ZooKeys 593: 1-14. DOI: 10.3897/zookeys.593.8511

Starobogatov Y.I., Sitnikova Y.T. 1990. Ways of mollusc speciation in Lake Baikal. Zhurnal Obshchey Biologii [Journal of General Biology] 4: 499-512. (in Russian)

Streelman J.T., Danley P.D. 2003. The stages of vertebrate evolutionary radiation. Trends in Ecology & Evolution 18: 126-131. DOI: 10.1016/S0169-5347(02)00036-8

Sun S., Li Q., Kong L. et al. 2017. Limited locomotive ability relaxed selective constraints on molluscs mitochondrial genomes. Scientific Reports 7: 1-8. DOI: 10.1038/s41598-017-11117-z

Tautz D., Renz M. 1983. An optimized freeze-squeeze method for the recovery of DNA fragments from agarose gels. Analytical Biochemistry 132: 14-19. DOI: 10.1016/0003-2697(83)90419-0

Templeton A.R., Crandall K.A., Sing C.F. 1992. A cladistic analysis of phenotypic associations with haplotypes inferred from restriction endonuclease mapping and DNA sequence data. III. Cladogram estimation. Genetics 132: 619-633.

Vinarski M.V., Kantor Y.I. 2016. Analytical catalogue of fresh and brackish water molluscs of Russia and adjacent countries. Moscow: Scintific Press Ltd KMK.

Veríssimo A., Zaera-Perez D., Leslie R. et al. 2017. Molecular diversity and distribution of eastern Atlantic and Mediterranean dogfishes Squalus highlight taxonomic issues in the genus. Zoologica Scripta 46: 414-428. DOI: 10.1111/zsc.12224

Wilke T. 2004. How dependable is a non-local molecular clock? A reply to Hausdorf et al. (2003). Molecular Phylogenetics and Evolution 30: 835. DOI: 10.1016/j.ympev.2003.08.008

Wilke T., Haase M., Hershler R. et al. 2013. Pushing short DNA fragments to the limit: Phylogenetic relationships of 'hydrobioid'gastropods (Caenogastropoda: Rissooidea). Molecular Phylogenetics and Evolution 66: 715-736. DOI: 10.1016/j.ympev.2012.10.025

Zubakov D.Y. 1999. Mollecular-phylogeny studying of the evolutionary history endemic baikalian molluscs families Baicaliidae and Benedictiidae (Gastropoda, Pectinibranchia). Cand. Sc. Dissertation, Institute of Cytology and Genetics, Novosibirsk, Russia. (in Russian)

Zubakov D.Y., Sherbakov D.Y., Sitnikova T.Y. 1997. Phylogeny of the endemial Baicaliidae molluscs inferred from partial nucleotide sequences of the CO1 mitochondrial gene. Molekulyarnaya Biologiya [Journal of Molecular Biology] 31: 935-939. (in Russian)